Plant Physiology Preview. Published on May 24, 2011, as DOI:10.1104/pp.110.168047

Running head: K^+, Mg^{2+}, and Ca^{2+} transport by OsHKT2;4 from *Oryza sativa*

Corresponding Author:

Julian I. Schroeder

Division of Biological Sciences, Cell and Developmental Biology Section

University of California, San Diego

La Jolla, CA 92093-0116, USA

Telephone number: 858-534-7759

Email address: julian@biomail.ucsd.edu

Research Category: Environmental Stress and Adaptation

K^+ transport by the OsHKT2;4 transporter from rice (*Oryza sativa*) with atypical Na^+ transport properties and competition in permeation of K^+ over Mg^{2+} and Ca^{2+} ions

Tomoaki Horie[1]*, Dennis E. Brodsky[2]*, Alex Costa[3], Toshiyuki Kaneko[4], Fiorella Lo Schiavo[3], Maki Katsuhara[4], Julian I. Schroeder[2+]

[1]Division of Applied Biology, Faculty of Textile Science and Technology, Shinshu University, 3-15-1, Tokita, Ueda, Nagano 386-8567, Japan

[2]Division of Biological Sciences, Cell and Developmental Biology Section, University of California, San Diego, 9500 Gilman Drive, La Jolla, CA 92093-0116, USA

[3]Dipartimento di Biologia, Università degli Studi di Padova, Via U. Bassi 58/B, 35131 Padova, Italy

[4]Institute of Plant Science and Resources, Okayama University, 20-1, Chuo-2-chome, Kurashiki, Okayama 710-0046, Japan

* These authors contributed equally to this research.

+ Corresponding author.

This research was supported by the grants from the Chemical Sciences, Geosciences, and Biosciences Division of the Office of Basic Energy Sciences at the US Department of Energy (DE-FG02-03ER15449 to J.I.S.), the National Institute of Health (grant no. ES010337 to J.I.S.), the Program for Promotion of Basic Research Activities for Innovative Biosciences (PROBRAIN), Japan (to M.K.), and by Grants in Aid for Scientific Research (23119507) from the Ministry of Education, Culture, Sports, Science, and Technology (T.H.).

Abstract

Members of the class II of HKT transporters, which have thus far only been isolated from grasses, were found to mediate Na^+-K^+ co-transport and at high Na^+ concentrations preferred Na^+-selective transport, depending on the ionic conditions. But the physiological functions of this K^+ transporting class II of HKT transporters remain unknown in plants with exception of the unique class II Na^+ transporter, OsHKT2;1. The genetically tractable rice (background Nipponbare) possesses two predicted K^+ transporting class II HKT transporter genes, *OsHKT2;3* and *OsHKT2;4*. In this study, we have characterized the ion selectivity of the class II rice (*Oryza sativa*) HKT transporter, OsHKT2;4, in yeast and *Xenopus laevis* oocytes. OsHKT2;4 rescued the growth defect of a K^+ uptake deficient yeast mutant. GFP-OsHKT2;4 is targeted to the plasma membrane in transgenic plant cells. OsHKT2;4-expressing oocytes exhibited strong K^+ permeability. Interestingly, however, K^+ influx in OsHKT2;4-expressing oocytes did not require stimulation by extracellular Na^+, in contrast to other class II HKT transporters. Furthermore, OsHKT2;4-mediated currents exhibited permeabilities to both Mg^{2+} and Ca^{2+}, in the absence of competing K^+ ions. Comparative analyses of Ca^{2+} and Mg^{2+} permeabilities in several HKT transporters, including AtHKT1;1, TaHKT2;1, OsHKT2;1, OsHKT2;2 and OsHKT2;4 revealed that only OsHKT2;4 and to a lesser degree TaHKT2;1 mediate Mg^{2+} transport. Interestingly, cation competition analyses demonstrate that the selectivity of both of these class II HKT transporters for K^+ is dominant over divalent cations, suggesting that Mg^{2+} and Ca^{2+} transport via OsHKT2;4 may be small and would depend on competing K^+ concentrations in plants.

Introduction

K^+ homeostasis is vital for growth and development of glycophytic plants. K^+ and Na^+ are chemically similar and are generally present at similar concentrations in non-saline soils. However, high concentrations of Na^+ over 100 mM can occur in arid/semi-arid environments and irrigated soils. Glycophytic plants selectively accumulate far more K^+ than Na^+ in the cytoplasm when the proportion of the two ions in the environment is similar (Flowers and Läuchli, 1983). K^+ taken up by roots is distributed to leaves. K^+ ions have diverse indispensable functions in plant cells including osmoregulation, cell expansion, enzyme activation, protein synthesis, membrane polarization and photosynthesis (Glass, 1983; Schroeder et al., 1994; Véry and Sentenac, 2003; Gierth et al., 2005). K^+ deficiency causes several deleterious effects including a decrease in cytosolic pH (Walker et al., 1996; Walker et al., 1998), resulting in substantial reductions in growth accompanied by damage to mature leaves and death of meristems (Flowers and Läuchli, 1983; Gierth and Mäser, 2007).

Multiple K^+ transport pathways across membranes contribute to the uptake and distribution of K^+ in plants, and many genes encoding channels and transporters that are permeable to K^+ have been identified in plants (Schroeder et al., 1994; Kwak et al., 2001; Lacombe et al., 2001; Véry and Sentenac, 2003; Gierth and Mäser, 2007; Lebaudy et al., 2007; Ward et al., 2009). The identified K^+ channels/transporters are presently classified into six families (Lebaudy et al., 2007; Ward et al., 2009).

Plant HKT transporters have mainly been characterized as monovalent cation transporters. The first characterized HKT transporter, TaHKT2;1, (Schachtman and Schroeder, 1994) from wheat was found to mediate Na^+-coupled K^+ transport and Na^+ transport at high Na^+ concentrations that occur under salinity stress conditions (Rubio et al., 1995; Gassmann et al., 1996). These findings suggested that other high-affinity K^+ uptake transporters must exist in roots, which were then identified as the KT/KUP/HAK transporter class (Quintero and Blatt, 1997; Santa-Maria et al., 1997; Fu and Luan, 1998; Kim et al., 1998; Gierth et al., 2005; Pyo et al., 2010). HKT transporters identified from many different plant species to date can be divided into 2 subgroups, class I and class II, based on phylogenetic analyses (Mäser et al., 2002b; Platten et al., 2006; Horie et al., 2009; Hauser and Horie, 2010) and largely correlating cation transport properties (Uozumi et al., 2000; Horie et al., 2001; Mäser et al., 2002b; Garciadeblás et

al., 2003; Yao et al., 2010).

Class I HKT transporters, including AtHKT1;1 from *Arabidopsis*, show a more Na^+ selective transport activity (Uozumi et al., 2000; Horie et al., 2001; Mäser et al., 2002b; Ren et al., 2005; Horie et al., 2009; Hauser and Horie, 2010). In contrast, class II HKT transporters including TaHKT2;1 show robust K^+ permeability. In recent years, most attention has focused on the Na^+ transporting HKT transporter properties and functions due to: (i) their unique Na^+ channel-like transport properties (Rubio et al., 1995; Gassmann et al., 1996; Liu et al., 2000; Horie et al., 2001; Ren et al., 2005; Corratgé et al., 2007; Jabnoune et al., 2009); (ii) the presence of class I HKT transporters with large Na^+ permeabilities (Uozumi et al., 2000; Horie et al., 2001; Jabnoune et al., 2009; Yao et al., 2010) and (iii) the central relevance of class I HKT Na^+ transporters for mediating salinity resistance in plants (Mäser et al., 2002a; Berthomieu et al., 2003; Ren et al., 2005; Sunarpi et al., 2005; Horie et al., 2006; Huang et al., 2006; Byrt et al., 2007; Davenport et al., 2007; Horie et al., 2009; Møller et al., 2009).

HKT transporters have been proposed to include four selectivity filter-pore-forming ("P-loop") domains, each sandwiched by two transmembrane domains, which are distantly homologous to the bacterial K^+ channel KcsA (Durell and Guy, 1999; Durell et al., 1999; Mäser et al., 2002). Furthermore, a glycine residue at the selectivity filter position in each P-loop, which corresponds to the first glycine of "the GYG motif" that is highly conserved among K^+ channels (Uozumi et al., 1995; Doyle et al., 1998), was found in HKT transporters (Durell and Guy, 1999; Mäser et al., 2002b; Hauser and Horie, 2010; Cao et al., 2011). Class I HKT transporters, however, were found to have a serine residue instead of this glycine residue at the filter position of the first P-loop region in contrast to class II HKT transporters retaining all four glycines at the four filter positions (Hauser and Horie, 2010). OsHKT2;1 from rice is a unique class II transporter that exhibits features of class I transporters such as conservation of this serine residue at the filter position of the first P-loop and poor K^+ permeability (Horie et al., 2001; Mäser et al., 2002b; Garciadeblás et al., 2003; Horie et al., 2007; Yao et al., 2010). Note that a non-selective alkali cation permeability and K^+ permeability of OsHKT2;1, was characterized using *Xenopus laevis* oocytes, in other research (Golldack et al., 2002). Biophysical transport analyses using *X. laevis* oocytes and yeast, expressing chimeric fusions and point-mutated DNA constructs of class I and class II HKT transporters, TaHKT2;1, AtHKT1;1, OsHKT2;1 and OsHKT2;2, demonstrated the contribution of the glycine residues in the four pore-loops to K^+ permeability of

class II HKT transporters (Mäser et al., 2002b; Tholema et al., 2005).

Whereas important Na^+-transporting functions of HKT transporters with a serine residue in the first P-loop have been identified *in planta* (Mäser et al., 2002a; Berthomieu et al., 2003; Sunarpi et al., 2005; Horie et al., 2006; Horie et al., 2007; Møller et al., 2009), the *in planta* function of the four glycine containing class II HKT transporters remain unknown. Multiple *HKT* genes were found in the *japonica* rice cultivar Nipponbare (Garciadeblás et al., 2003). Seven full length *OsHKT* transporter genes were identified, consisting of four class I transporters and three class II transporters including OsHKT2;1 (Horie et al., 2001; Garciadeblás et al., 2003; Platten et al., 2006). OsHKT2;3 and OsHKT2;4 are the most closely related among all analyzed HKT transporters, and share approximately 93% identity at the amino acid sequence level. OsHKT2;3 and OsHKT2;4 are the only class II transporters that conserve glycines at the four pore-loop filter positions in Nipponbare. An additional *OsHKT2;2* gene encoding a K^+-permeable class II transporter was isolated from a salt tolerant *indica* cultivar, Pokkali (Horie et al., 2001) and expression in plant cells exhibited Na^+-coupled K^+ transport (Yao et al., 2010), confirming previous cation selectivity studies in yeast and *Xenopus* oocytes (Horie et al., 2001). OsHKT2;2 is a non-full length pseudogene in Nipponbare (Garciadeblás et al., 2003). Thus OsHKT2;3 and OsHKT2;4 provide the only class II HKT transporters in the genetically tractable Nipponbare rice background. However, first their cation selectivity properties need to be analyzed.

In the present study we have analyzed the ion selectivity of OsHKT2;4 using yeast and *X. laevis* oocytes. We show that OsHKT2;4 is targeted to the plasma membrane in transgenic plant cells and that OsHKT2;4 exhibits a robust K^+ permeability in both expression systems. Interestingly, however, OsHKT2;4 did not show Na^+-coupled K^+ transport unlike other class II HKT transporters and OsHKT2;4-mediated K^+ transport is shown here to be Na^+ independent. Moreover, OsHKT2;4 exhibits a smaller Na^+ conductance compared to TaHKT2;1 and the other HKT transporters analyzed in the present study. OsHKT2;4 expressed in *X. laevis* oocytes has recently been found to exhibit permeability to a wide range of cations including divalent cations such as Ca^{2+} and Mg^{2+} (Lan et al., 2010). Here, independent analysis of Ca^{2+} and Mg^{2+} permeabilities among five plant HKTs: AtHKT1;1, TaHKT2;1, OsHKT2;1, OsHKT2;2 and OsHKT2;4, in *X. laevis* oocytes reveal that TaHKT2;1 shows a small Mg^{2+} permeability. In contrast, OsHKT2;4 exhibits permeability for both Mg^{2+} and Ca^{2+}. Competition experiments however show, that both OsHKT2;4 and TaHKT2;1 exhibit stronger selectivity for the

monovalent cation K^+, which out-competes Ca^{2+} and Mg^{2+} transport.

Results

Functional expression of OsHKT2;3 and OsHKT2;4 in yeast

The OsHKT2;3 and OsHKT2;4 transporters retain the four selectivity filter Gly residues, typical of class II HKT transporters (Schachtman and Schroeder, 1994; Garciadeblás et al., 2003; Horie et al., 2009; Hauser and Horie, 2010). We therefore expressed OsHKT2;3 and OsHKT2;4 in a high-affinity K^+-uptake-deficient mutant of yeast strain, CY162 (Anderson et al., 1992), and performed growth analyses under K^+-limited conditions. All transformants showed no remarkable difference in their growth when K^+ was supplied at a high 10 mM concentration (Fig. 1A). However, only the expression of OsHKT2;4 and OsHKT2;2 could rescue the growth defect of the mutant in the presence of 0.1 mM KCl (Fig. 1B). OsHKT2;3, which shows more than 93% identity to OsHKT2;4 at the amino acid sequence level, did not complement the mutations (Fig. 1B).

The TaHKT2;1 transporter from wheat has been shown to exhibit low-affinity Na^+ transport with Na^+-channel-like transport properties in the presence of high Na^+ concentrations in yeast (Rubio et al., 1995; Gassmann et al., 1996; Rubio et al., 1999), and similar Na^+ transport properties were found for OsHKT2;1 and OsHKT2;2 (Horie et al., 2001; Yao et al., 2010). Therefore, we next expressed OsHKT proteins in a Na^+ hypersensitive mutant yeast strain, G19 (Rubio et al., 1999). Increasing the concentration of NaCl in the growth medium caused severe growth defects in OsHKT2;1-expressing cells compared with vector-harboring control cells as previously reported (Horie et al., 2001) (Fig. 2A-D). In comparison, G19 cells expressing the K^+-permeable transporters, OsHKT2;2 and OsHKT2;4, were able to grow on medium containing 200 mM NaCl although OsHKT2;2-expressing cells exhibit remarkably greater sensitivity to NaCl stress. In contrast, control cells no longer survived (Fig. 2D). OsHKT2;3-harboring cells exhibited very similar Na^+ sensitivity to control cells (Fig. 2A-D).

Monovalent alkali cation selectivity of OsHKT2;4 in *Xenopus laevis* oocytes

To investigate ion selectivity properties of class II HKT transporters, two-electrode

voltage clamp experiments using *X. laevis* oocytes were performed. OsHKT2;3- and OsHKT2;4-dependent currents were recorded by exposing each *OsHKT2* cRNA-injected oocyte to bath solutions, supplemented with 10 mM alkali cation salts. Control water-injected oocytes showed small background currents (Fig. 3A). In the case of *OsHKT2;3* cRNA-injected oocytes, none of the alkali cations evoked significant currents that differed from water-injected control oocytes (data not shown). In contrast, however, *OsHKT2;4* cRNA-injected oocytes showed large currents for every alkali cation tested (Fig. 3A and supplementary Figure 1). OsHKT2;4-mediated currents shared an inward rectification for all cations tested (Fig. 3A and supplementary Figure 1). Among the five alkali cations, K^+ showed the most positive reversal potential, followed by $Rb^+ \cong Cs^+$ and $Na^+ \cong Li^+$, suggesting a higher relative K^+ permeability compared to other alkali cations (Fig. 3A). Given that HKT transporters exhibit characteristic Na^+ uniport activity at high Na^+ concentrations, amplitudes of OsHKT2;4-mediated inward currents were compared with those of OsHKT2;1 and OsHKT2;2 at voltages negative of -150 mV, recorded with 10 mM NaCl in the bath solution. The results revealed substantial differences in current magnitudes in response to 10 mM NaCl between OsHKT2;4 and the other two class II OsHKT transporters (Fig. 3B).

The class II HKT transporters with four glycine residues in their selectivity filter domains characterized to date show Na^+-K^+ co-transport (Rubio et al., 1995; Yao et al., 2010). We thus analyzed the combined effects of Na^+ and K^+ on OsHKT2;4-expressing oocytes to determine whether OsHKT2;4 can mediate similar Na^+-K^+ co-transport. In the first type of experiments, OsHKT2;4-mediated currents were recorded in bath solutions where Na^+ was set to 0.3 mM and the K^+ concentration was increased from 0.3 mM to 10 mM. The current (I) - voltage (V) relationships of OsHKT2;4-expressing oocytes revealed significant positive shifts in the reversal potential and increases in inward currents as the K^+ concentration of the bath solution was increased (Fig. 4A), exhibiting a clear K^+ permeability. In contrast, the I-V relationship of OsHKT2;4-expressing oocytes bathed with constant 0.3 mM K^+ with increasing Na^+ concentrations exhibited only slight positive reversal potential shifts such that increases in the extracellular Na^+ concentration from 0.3 mM to 3.0 mM and 10 mM led to approximately +9 mV and +5 mV reversal potential shifts, respectively, in comparison with 0.3 mM extracellular Na^+ concentration (Fig. 4B). The transport properties of OsHKT2;4 showed marked differences to other class II plant HKT transporters characterized thus far which showed much larger and

increasing positive shifts in the reversal potential upon increasing extracellular Na^+ concentration (Rubio et al., 1995; Gassmann et al., 1996; Liu et al., 2000; Horie et al., 2001; Yao et al., 2010).

Serial dilutions showed K^+-dependent growth complementation of yeast expressing either OsHKT2;2 or OsHKT2;4 in the absence of Na^+ stress (Fig. 5A-B). The difference in K^+/Na^+ selectivities of K^+-transporting OsHKT2 transporters was further evaluated using CY162 cells. OsHKT2;4-expressing cells exhibited less sensitivity to high concentrations of NaCl compared to OsHKT2;2-expressing cells in the presence of 0.1 mM KCl (Fig. 5A). A tenfold increase in the K^+ concentration in the medium remarkably strengthened the growth of OsHKT2;4-expressing cells under high NaCl concentrations in contrast to the case of OsHKT2;2-expressing cells (Fig. 5B).

We further analyzed OsHKT2;4-mediated K^+ currents by exposing OsHKT2;4-expressing oocytes to increasing extracellular K^+ concentrations with no added extracellular Na^+. Increasing the K^+ concentration from 0.3 mM to 10 mM resulted in significant positive shifts in the reversal potential (Fig. 6). Reversal potentials shifted by approximately +18 mV when the extracellular K^+ concentration was increased from 0.3 mM to 3 mM (Fig. 6). These data provide clear evidence that OsHKT2;4 transports K^+ and is not an obligate Na^+-K^+ co-transporter.

To predict an approximate apparent affinity of OsHKT2;4 for K^+, complementation tests using CY162 cells were performed. OsHKT2;4-expressing cells were able to grow in the presence of more than 25 μM K^+ (Fig. 7A). However, growth of OsHKT2;4-expressing cells was weaker than that of OsHKT2;2-expressing cells, particularly when extracellular K^+ concentrations were lower than 50 μM (Fig. 7A). On the other hand, OsHKT2;4-expressing cells showed more robust growth than OsHKT2;2-expressing cells at 1 mM K^+ (Fig. 7A). The growth of OsHKT2;4-expressing cells in liquid AP medium supplemented with either 25, 50, 75, 100, 250, 500 or 1000 μM K^+ was monitored by measuring OD_{600}. Regression analyses were performed for OsHKT2;4-expressing cells at the logarithmic growth phase. Resultant slope values were plotted (Fig. 7B). Michaelis-Mention analysis approximated an apparent affinity for OsHKT2;4-mediated K^+ influx of about 300 μM (R^2=~0.875). We analyzed the data with two components and the R^2 value was not improved.

Divalent cation selectivity of HKT transporters in *Xenopus laevis* oocytes

During the above experiments, we noticed unusual shifts in the reversal potentials of

OsHKT2;4-mediated currents, including when $MgCl_2$ and Mg-Glutamate concentrations were changed. Recently, OsHKT2;4 was independently reported to be a cation transporter showing substrate specificity to a wide range of cations including Ca^{2+} and Mg^{2+} (Lan et al., 2010). Based on our initial observations and this recent report, we next analyzed several members of the HKT family for Mg^{2+} and Ca^{2+} transport properties (Fig. 8). Each HKT protein was exposed to 5 mM and high 50 mM concentrations of Mg^{2+} and Ca^{2+}, as chloride salts, in the bath solution. The same conditions were also applied to water-injected oocytes as a control. As no significant differences in the resulting inward currents of water-injected control oocytes were observed, all control oocytes were combined into one group for simplicity (Fig. 8). Electrophysiological recordings were performed using both voltage pulse and voltage ramp protocols with similar findings, and the voltage ramp recordings were used to generate the current-voltage graphs in Figure 8 with representative voltage pulse response time-dependent recordings shown in Figure 9.

For the AtHKT1;1, OsHKT2;1, and OsHKT2;2 transporters (Uozumi et al., 2000; Horie et al., 2001), no significant differences in the current magnitudes were observed when the extracellular Mg^{2+} concentrations were increased from 5 mM to 50 mM (Fig. 8A-C; $P \geq 0.114$ at -150 mV; Wilcoxon Signed Rank Test). The shifts in reversal potentials upon these tenfold-increases in Mg^{2+} concentration were +1 mV for AtHKT1;1, +4 mV for OsHKT2;1, and +13 mV for OsHKT2;2. Note that this +13 mV shift in reversal potential indicates a small relative Mg^{2+} permeability of OsHKT2;2 (Fig. 8C). OsHKT2;4 and TaHKT2;1, on the other hand, showed larger ion currents and positive reversal potential shifts upon increasing the extracellular Mg^{2+} concentration (Fig. 8D-E). For OsHKT2;4-mediated currents, an average +33 mV reversal potential shift was observed when increasing the extracellular $MgCl_2$ concentration from 5 mM to 50 mM. Moreover, an average +45 mV shift in the reversal potential of OsHKT2;4-dependent currents was observed when increasing the extracellular concentration of $CaCl_2$ from 5 to 50 mM. These results suggest that OsHKT2;4 is highly permeable to Mg^{2+} and Ca^{2+}. A +45 mV shift for a tenfold Ca^{2+} concentration increase also suggests that in addition to Ca^{2+} permeability, Ca^{2+} itself modulates other ion conductances in oocytes, possibly in the form of activating endogenous Ca^{2+}-activated Cl^- channels (Cao et al., 1995), setting the reversal potential closer to the calculated chloride reversal potential (E_{Cl}) of -23 mV in a 50 mM $CaCl_2$ bath solution, assuming an internal Cl^- concentration of 40 mM in oocytes (Barish, 1983). The calculated

chloride equilibrium potential with 5 mM $CaCl_2$ was approximately +34 mV. For the wheat transporter TaHKT2;1, reversal potentials shifted less dramatically, exhibiting an average shift of +20 mV with the same tenfold increase in $MgCl_2$ concentration. Upon increasing the $CaCl_2$ concentration, however, the reversal potential shift was negligible with an average shift of -2 mV (Fig. 8E). These results indicate Mg^{2+} permeability, but not a substantial Ca^{2+} permeability under these conditions. The lack of a clear measured shift in reversal potential with Ca^{2+} increases for TaHKT2;1 is consistent with previous results from unpublished pilot studies (W. Gassmann and Schroeder, unpublished observations). Nevertheless larger average inward currents were observed at 50 mM $CaCl_2$, indicating a possible small effect of Ca^{2+} on TaHKT2;1-dependent transport. Relative permeability ratios for OsHKT2;4 (P_{Mg}/P_K of 0.0203 and P_{Ca}/P_K of 0.0108) and TaHKT2;1 (P_{Mg}/P_K of 0.0187) were determined (Fatt and Ginsborg, 1958) using reversal potentials of OsHKT2;4-mediated currents from Figure 8, and assuming an intracellular K^+ concentration of 100 mM (Schroeder et al., 1994). These results indicate a much stronger permeability towards K^+ than to either of the divalent cations, for both transporters. Note however, that this does not rule out uptake of Ca^{2+} or Mg^{2+} via OsHKT2;4 or TaHKT2;1 down a relatively steep electrochemical gradient, depending on the relative competition among permeating cations. Analyses of the time-dependence of OsHKT2;4- and TaHKT2;1-mediated currents in response to voltage pulses showed differences between the two transporters (Fig. 9). Increases in whole-cell currents in oocytes expressing TaHKT2;1 in the presence of high 50 mM $CaCl_2$ indicate a possible small Ca^{2+} permeability of TaHKT2;1, and a possible contribution to currents by endogenous Ca^{2+} activated Cl^- channels in oocytes (Figs. 8E and 9). Furthermore, OsHKT2;4-mediated currents exhibited a time-dependent activation at more negative voltages, in contrast to TaHKT2;1-mediated currents (Fig. 9).

Previous studies on animal Ca^{2+} channels have shown the appearance of a large Na^+ conductance when extracellular Ca^{2+} is removed, showing that Ca^{2+} outcompetes Na^+ selectivity in voltage-dependent Ca^{2+} channels (Almers et al., 1984; Hille, 1992). Na^+ or K^+ competition experiments with Mg^{2+} and Ca^{2+} were performed to determine the preference in cation permeabilities of OsHKT2;4 and TaHKT2;1 for monovalent and divalent cations (Fig. 10). OsHKT2;4-expressing oocytes were exposed to 10 mM K^+ while TaHKT2;1 was analyzed with 10 mM Na^+/3 mM K^+ for the competition experiments, as these conditions trigger inward cation currents in the respective HKT transporters (Figs. 3A and 6) (Rubio et al., 1995). For

OsHKT2;4-mediated currents, the reversal potential shifted by only +5 mV upon addition of 50 mM Mg^{2+} to the bath solution (Fig. 10A). Similarly, the reversal potential shifted by +4 mV upon addition of 50 mM Ca^{2+} to the bath solution (Fig. 10A). The average inward current magnitudes in the presence of 10 mM K^+ plus 50 mM Mg^{2+} or 50 mM Ca^{2+} groups were slightly larger than 10 mM K^+ alone, and these increases were not statistically significant at -150 mV (Fig. 10A; $P > 0.095$; Wilcoxon Signed Rank Test). These results indicate that Mg^{2+} and Ca^{2+} were substantially less permeable under competing 10 mM K^+ conditions, despite the high (50 mM) divalent cation concentrations tested. A small residual permeation of Mg^{2+} or Ca^{2+} may however occur. When TaHKT2;1-expressing oocytes were exposed to 50 mM added Mg^{2+} in competition experiments, the reversal potential shifted by +6 mV. When 50 mM Ca^{2+} was added to the bath solution, the reversal potential shifted +3 mV. Average inward current magnitudes in the presence of 10 mM Na^+/3 mM K^+ plus 50 mM Mg^{2+} or 50 mM Ca^{2+} groups were also slightly larger than 10 mM Na^+/3 mM K^+ alone, and the increases were statistically significant at -150 mV (Fig. 10B; $P < 0.005$; Wilcoxon Signed Rank Test). Although the differences in ion conductance under the described competition settings were found to be significant for TaHKT2;1 using a paired and ranked statistical test, they were not large. These findings together show a competitive inhibition of the ability of these HKT transporters to transport Ca^{2+} and Mg^{2+} in the presence of permeating K^+ and Na^+ cations, even when high 50 mM [Mg^{2+}] or [Ca^{2+}] were extracellularly added to the 10-13 mM total [K^+] and [Na^+].

Additional experiments were performed for OsHKT2;4-expressing oocytes in which 5 mM Ca^{2+} was added to the bath solution in the presence of K^+ concentrations ranging from 0 to 10 mM K^+. We found that as the extracellular concentration of bath K^+ was increased, the reversal potentials were shifted to more positive voltages. When 0.1 mM K^+ was added to the bath solution containing 5 mM Ca^{2+}, the reversal potential shifted -2 mV. However, when larger concentrations of K^+ were added to the bath, a clear trend of positive reversal potential shifts was observed. When 1 mM K^+ was added to the bath solution, the reversal potential shifted +16 mV, and after 10 mM K^+ was added to the bath solution, the reversal potential shifted +36 mV compared to the 5 mM $CaCl_2$ bath solution. These findings highlight the ability of OsHKT2;4 to transport K^+ in the presence of competing Ca^{2+}.

Subcellular localization of OsHKT2;4 in plant cells

To determine the membrane localization of the OsHKT2;4 protein in plant cells, we constructed OsHKT2;4 fused with EGFP at the N-terminus (EGFP-OsHKT2;4). Localization analyses were performed using protoplasts of *Arabidopsis* mesophyll cells. Figure 11A-C shows protoplasts expressing the EGFP-OsHKT2;4 protein. The GFP fluorescence signal was uniformly present at the periphery of the cell (Fig. 11A and C). A small fluorescence signal was also detected inside cells, which may reflect endoplasmic reticulum localization, where the protein is assembled (Fig. 11A). As controls, we transformed protoplasts with free EGFP which showed the typical cytoplasmic and nuclear localizations (Fig. 11D-F). To better determine whether OsHKT2;4 shows plasma membrane localization, we stained protoplasts expressing EGFP-OsHKT2;4 with the plasma membrane marker FM4-64 (Fig. 11G-I) (Bolte et al., 2004; Horie et al., 2007). The green and red fluorescence signals from EGFP and FM4-64 in protoplasts expressing the EGFP-OsHKT2;4 protein (Fig. 11G and H) uniformly overlapped when the two images were combined (Fig. 11I). In comparison, when the same staining was performed with protoplasts expressing the free EGFP, a clear overlap of the two signals was not observed (Fig. 11J-L). In the confocal plane shown in figure 11J, the EGFP signal appeared to also be present at the periphery of the cell. This was due to the presence of the large central vacuole, which pushed the cytoplasm towards the plasma membrane. Together, these results provide evidence that EGFP-OsHKT2;4 localizes to the plasma membrane of *Arabidopsis* mesophyll protoplasts, suggesting plasma membrane localization of OsHKT2;4 in plant cells.

Discussion

HKT transporters are one of the best characterized cation transporters in plants. TaHKT2;1 was isolated by complementation screening of a K^+ starvation-treated wheat root library using a high-affinity K^+ uptake deficient mutant of yeast (Schachtman and Schroeder, 1994). Initial *X. laevis* oocytes voltage clamp analyses showed that all alkali cations tested affected TaHKT2;1-mediated outward currents (Schachtman and Schroeder, 1994). Subsequent ion selectivity analyses of TaHKT2;1-induced inward currents expressed in *X. laevis* oocytes and K^+ and Na^+ flux analyses in yeast revealed that TaHKT2;1 mediates high-affinity Na^+-K^+ co-transport and also exhibits Na^+-selective low-affinity channel-like Na^+ transport in the presence

of mM concentrations of Na^+ (Rubio et al., 1995; Gassmann et al., 1996). Complementary DNAs encoding HKT transporter family members have been identified in many plant species and the monovalent cation transport properties of the encoded proteins have been characterized, mainly in heterologous expression systems (Gassmann et al., 1996; Rubio et al., 1999; Liu et al., 2000; Horie et al., 2001; Liu et al., 2001; Garciadeblás et al., 2003; Horie et al., 2009; Hauser and Horie, 2010), and in a few exceptions in plant cells (Laurie et al., 2002; Horie et al., 2007; Yao et al., 2010). These analyses have shown that class I HKT transporters and OsHKT2;1 preferentially show Na^+ transport activity (Uozumi et al., 2000; Horie et al., 2001; Mäser et al., 2002; Garciadeblás et al., 2003; Jabnoune et al., 2009; Yao et al., 2010).

Phylogenetic analyses of the identified HKT proteins showed that HKT transporters can be divided into at least two subgroups: class I and class II transporters, which show preferred Na^+ selective transport in class I transporters, and K^+ transport as well as Na^+ transport for class II HKT transporters (Mäser et al., 2002b; Platten et al., 2006; Horie et al., 2009; Hauser and Horie, 2010). Molecular genetic research demonstrated that the Na^+ transport activity mediated by members of the class I HKT transporter plays a key role in Na^+-tolerance and in Na^+ exclusion from leaves in *Arabidopsis*, rice, and wheat (Mäser et al., 2002a; Berthomieu et al., 2003; Ren et al., 2005; Sunarpi et al., 2005; Horie et al., 2006; Huang et al., 2006; Byrt et al., 2007; Davenport et al., 2007; Møller et al., 2009). Furthermore, OsHKT2;1, a unique class II transporter that mediates more Na^+ selective transport and lacks substantial K^+ permeability (Horie et al., 2001; Yao et al., 2010), unlike the other typical class II transporters, has been shown to compensate for K^+ deficiency through nutritional root Na^+ uptake and distribution in rice plants (Horie et al., 2007).

Compared to class I HKT transporters, little information exists on the functions of K^+ transporting class II HKT transporters *in planta*. Thus far class II HKT transporters have only been identified in grasses, including wheat, rice, barley, and common reed (*Phragmites australis*) (Schachtman and Schroeder, 1994; Wang et al., 1998; Takahashi et al., 2007; Huang et al., 2008). In this study, we analyzed the cation selectivity properties of the OsHKT2;4 transporter, surprisingly showing that OsHKT2;4 exhibits a distinct ion selectivity for K^+ and Na^+ in comparison with other HKT transporters. OsHKT2;4 mediates robust inward K^+ currents, even without addition of extracellular Na^+, unlike other class II HKT transporters (Figs. 3A, 4, 6, 10 and Supplementary Figure 1), implying that OsHKT2;4 plays a role in K^+ homeostasis as a K^+

transporter/channel rather than a Na^+-K^+ co-transporter. The K^+-permeable class II HKT transporters were found to retain a glycine residue at each filter position in the four selectivity pore-forming regions that have been proposed to be derived from an ancestral K^+ channel in bacteria (Durell and Guy, 1999; Durell et al., 1999; Mäser et al., 2002b; Tholema et al., 2005). Ion transport analyses of plant HKTs and of the bacterial HKT homolog, KtrAB K^+ transport system, from *Vibrio alginolyticus*, demonstrated that the glycines at the filter positions are important contributors to robust K^+ transport via HKT transporters (Mäser et al., 2002b; Tholema et al., 2005). OsHKT2;3 and OsHKT2;4 transporters are the only two full-length class II transporters found in the genetically tractable *japonica* rice cv. Nipponbare genome, in which all four glycines at the selectivity filter positions are conserved. Moreover, OsHKT2;3 and OsHKT2;4 show more than 93% identity at the amino acid sequence level. The expression of OsHKT2;3 did not cause any difference in the growth response of either CY162 or G19 mutant yeast cells compared to vector-harboring control cells (Figs. 1 and 2). Furthermore, no significant OsHKT2;3-mediated currents were observed in various cation solutions in comparison with water-injected control oocytes in two electrode voltage clamp experiments (data not shown). Note that the sequences of expression constructs in yeast and oocytes were carefully checked and found to possess no errors. Transient expression of EGFP-OsHKT2;3 revealed a plasma membrane localization of the chimeric protein in protoplasts of *Arabidopsis* mesophyll cells (Supplementary Figure 2) as found in similar analyses for EGFP-OsHKT2;4 expression construct (Fig. 11). These results suggest that OsHKT2;3 may not localize correctly or may not exhibit ion transport activity in heterologous cells, for unknown reasons. Further investigations into OsHKT2;3, including subcellular localization in heterologous cells and co-expression with OsHKT2;4, will be needed to elucidate its physiological functions. The expression of OsHKT2;4 triggered robust growth responses in yeast cells and elicited significant currents in oocytes (Figs. 1 to 10 and Supplementary Figures 1 and 3).

K^+ uniport function of OsHKT2;4 in yeast and *X. laevis* oocytes

The expression of OsHKT2;4 rescued growth defects of CY162 yeast cells that are deficient in high-affinity K^+ uptake (Fig. 1B), similar to other typical class II HKT transporters such as TaHKT2;1 and OsHKT2;2 (Schachtman and Schroeder, 1994; Horie et al., 2001). Robust K^+ permeability was also found in oocytes expressing OsHKT2;4 (Figs. 3A, 4A and 6). However,

a remarkable distinction was found in the Na^+ transport properties between OsHKT2;4 and the HKT transporters characterized to date. OsHKT2;4-mediated Na^+ transport activity at high extracellular Na^+ concentrations appears to be smaller in comparison to that of OsHKT2;1 and OsHKT2;2 (Fig. 3B). Increasing Na^+ concentrations in a 0.3 mM K^+ bath solution caused only slight positive shifts in the reversal potential of OsHKT2;4-expressing oocytes (Fig. 4B). Furthermore, OsHKT2;4-expressing G19 yeast cells showed the lowest sensitivity to extracellular NaCl, even lower than vector-harboring control cells (Fig. 2). OsHKT2;4 shows strong K^+ uptake complementation activity, suggesting robust functional expression in yeast (Fig. 1B). High-affinity K^+ uptake deficient CY162 cells also exhibited less sensitivity to NaCl upon expression of OsHKT2;4, in comparison with the expression of OsHKT2;2, consistent with functional OsHKT2;4 expression (Fig. 5). The increased salt tolerance of yeast cells expressing OsHKT2;4 may be due to an increased K^+ accumulation via OsHKT2;4 and less Na^+ transport compared to OsHKT2;2 (Figs. 2 and 5), based on previous studies of Na^+ sensitivities of HKT-expressing yeast lines (Rubio et al., 1995; Rubio et al., 1999; Yenush et al., 2002). Previous studies on OsHKT2;2 expressed in tobacco cultured BY2 cells predicted an apparent affinity for OsHKT2;2-mediated Rb^+ (K^+) influx of approximately 35 μM (Yao et al., 2010). The growth assay-based prediction of an apparent affinity for OsHKT2;4-mediated K^+ influx led to an apparent K_m of approximately 300 μM K^+ (Fig. 7). Higher affinity of OsHKT2;2-mediated K^+ influx than that mediated by OsHKT2;4 is also consistent with complementation analyses under low extracellular K^+ concentrations, for example at 10 to 25 μM K^+ (Fig. 7A). Taken together, the present findings show that OsHKT2;4 has a distinct K^+/Na^+ selectivity compared to other class II HKT transporters with four glycine residues such that OsHKT2;4 mediates robust channel-like K^+ uniport independent of Na^+.

Recent voltage clamp analyses of OsHKT2;4-expressing oocytes have indicated that OsHKT2;4 mediates transport of various cations, including divalent cations such as Ca^{2+} and Mg^{2+} (Lan et al., 2010). Together with plasma membrane localization of OsHKT2;4 in root hair cells of rice cv. Nipponbare plants, a novel physiological role of OsHKT2;4 in Ca^{2+}-related biological processes other than K^+/Na^+ homeostasis was implicated (Lan et al., 2010). Independent experiments in the present study in which extracellular $MgCl_2$ or $CaCl_2$ was added showed correlating shifts in the reversal potential. Here, we thus analyzed Ca^{2+} and Mg^{2+} selectivity among five HKT transporters, TaHKT2;1, AtHKT1;1, OsHKT2;1, OsHKT2;2 and

OsHKT2;4. In addition to the confirmation of Ca^{2+} and Mg^{2+} permeabilities of OsHKT2;4 as reported (Lan et al., 2010), TaHKT2;1 was found to show a permeability for Mg^{2+}, and a possible but small effect of Ca^{2+} on ionic currents (Fig. 8D-E). To gain insight into the significance of divalent cation transport activity by OsHKT2;4 and TaHKT2;1, competition experiments were performed in the presence of primary monovalent and divalent cation substrates. OsHKT2;4 and TaHKT2;1 both showed very small divalent cation permeabilities when 50 mM Ca^{2+} or Mg^{2+} were added to Na^+ and/or K^+ containing bath solutions (Fig. 10A-B). Increases in the K^+ concentration from 0.1 to 1 mM and to 10 mM in the presence of 5 mM $CaCl_2$ cause positive shifts in the reversal potential, consistent with these findings. These results suggest that these HKT transporters favor transport of K^+ over Ca^{2+} and Mg^{2+}. Thus, given the abundance of K^+ in plant cells, the physiological functions of OsHKT2;4 will depend strongly on the ionic conditions and the cell types in which OsHKT2;4 is expressed. Whether significant OsHKT2;4-mediated Ca^{2+} or Mg^{2+} transport activities occur *in vivo* in rice will need to be analyzed *in planta*, using rice knock out lines, similar to OsHKT2;1 analyses (Horie et al., 2007).

The *OsHKT2;4* gene was reported to be diversely expressed in rice plants, including leaf sheaths and primary/lateral roots (Lan et al., 2010). Our findings suggest that OsHKT2;4 functions as a K^+-permeable transporter/channel with a smaller and permeability to Ca^{2+} and Mg^{2+}, that is competitively inhibited by K^+. We have isolated two independent *oshkt2;4* rice knock out lines from the *Tos17* mutant population (Hirochika et al., 1996; Miyao et al., 2003; Horie et al., 2007), but no profound phenotype to various ionic conditions has been observed thus far (unpublished data). OsHKT2;4 is highly identical to OsHKT2;3, including their 5' UTRs which also show conservation, and they may cooperatively function *in vivo* in rice plants. Further investigations of not only *oshkt2;4* single mutants but *oshkt2;3* single and *oshkt2;3 oshkt2;4* double mutants could contribute to the understanding of the physiological roles of OsHKT2;4 in rice plants. Moreover, given the numerous studies analyzing the monovalent cation transporting properties of HKT transporters, and only two studies reporting analyses of divalent cation transport properties of HKT transporters (Lan et al., 2010 and the present study), further studies on the regulation and ion selectivities of both OsHKT2;3 and OsHKT2;4 will be important for assessing their biological functions.

Materials and Methods

Expression of OsHKTs in Yeast.

All *OsHKT* cDNAs were subcloned downstream of the *Gal1* promoter in the plasmid pYES2 (Invitrogen). The K^+ uptake deficient CY162 [*MAT*a, *Δtrk1*, *trk2*::pCK64, *his3*, *leu2*, *ura3*, *trp1*, *ade2*] (Anderson et al., 1992) and the Na^+ sensitive G19 [*MAT*a, *his3*, *leu2*, *ura3*, *trp1*, *ade2*, *ena1::HIS3::ena4*] (Quintero et al., 1996) *Saccharomyces cerevisiae* strains were used. Selection of transformants and subsequent growth assays using an arginine phosphate (AP) medium (Rodríguez-Navarro and Ramos, 1984) were performed as described previously (Rubio et al., 1999; Horie et al., 2001). Briefly, for both complementation and Na^+ sensitivity analyses, AP media supplemented with 0.8 g/liter CSM-ura (Bio101), 2% (w/v) galactose, 0.6% (w/v) sucrose, 2% (w/v) agar, and the indicated concentrations of KCl and NaCl were used. As for the growth assays using AP plates with serial dilutions or liquid AP medium, each CY162 transformant was pre-cultured in the liquid Synthetic Complete (SC)-Uracil medium supplemented with 50 mM KCl at 30°C for 1 day. One ml of each culture solution was centrifuged at 8000 rpm for 1 min and supernatant was removed. Cells were washed with the liquid AP medium with no added K^+ and Na^+ for three times and diluted in the same AP medium with the approximate OD_{600} of 1.0. These samples were used to make 1:10 serial dilutions, which were subsequently spotted onto each plate, starting with 10^{-1} dilutions. For the measurement of OD_{600}, the washed cell samples were directly used for inoculation into 5 ml of each K^+-supplied liquid AP medium. Three independent clones per construct were analyzed in all growth tests on solid medium and plates were incubated at 30°C for 4 to 10 days. One independent clone was used for the measurement of OD_{600} using the liquid AP medium.

OsHKT expression constructs and electrophysiology in *X. laevis* oocytes

For the synthesis of *TaHKT2;1*, *OsHKT2;1* and *OsHKT2;2* cRNA, previously reported constructs were used (Schachtman and Schroeder, 1994; Horie et al., 2001). *OsHKT2;3*, *OsHKT2;4* and *AtHKT1;1* cDNAs were subcloned into the pXβG-ev1 vector (Preston et al., 1992). Each cRNA was transcribed from linearized plasmid constructs using the mMESSAGE mMACHINE *in vitro* transcription kit (Ambion).

Oocytes were kept for 1 to 3 d at 18°C in either a ND-96 solution or a modified Barth's

solution. Approximately 50 ng of cRNA, in a total volume of 50 nl, was injected into each *Xenopus laevis* oocyte for voltage clamp recordings. Recordings were performed 1-3 days after injection.

For the experiments shown in figures 3 to 5, voltage clamp recordings were performed using a dual-electrode voltage clamp amplifier (Nihon Kohden). Oocytes were perfused with a solution containing 6 mM $MgCl_2$, 1.8 mM $CaCl_2$, 10 mM MES-BTP, pH 5.5, 180 mM D-mannitol, and the indicated concentrations of Na- and K-Glutamate or 10 mM alkali cations as chloride salts. The ionic strength was kept constant by adding Tris-Glutamate. Lab-Trax-4/16 (World Precision Instruments) was used for electrophysiological measurements and voltage steps were applied from 0 to -150 mV in -15 mV decrements with a holding potential of -40 mV as described previously (Yao et al., 2010). A 3 M KCl agar bridge was used as a bath electrode.

For experiments shown in figures 6 to 8, recordings were performed with a Cornerstone (Dagan; Minneapolis, MN) TEV-200 two-electrode voltage clamp amplifier. Data analyses were performed using an Axon Instruments Digidata 1440A Low-Noise Data Acquisition System (Molecular Devices; Sunnyvale, CA). Oocytes were subjected to voltage pulses to record time-dependent currents (Schroeder, 1989) and to voltage ramps, with a holding potential of -40 mV. Data were low-pass filtered at 50 Hz throughout all recordings. Oocytes were bathed in 10 mM Tris, 0.3 mM EGTA (except in solutions containing calcium). The indicated concentrations of $MgCl_2$, $CaCl_2$, NaCl, and KCl, were added at pH = 7.4 (with Tris base, glutamic acid, or HCl) and osmolalities were adjusted to 220-260 mosmol/kg with D-mannitol. Two different pH conditions were used depending on the experiments in this study. Note that changes in the extracellular pH did not cause significant effects on reversal potentials or Mg^{2+} currents of OsHKT2;4-expressing oocytes in a 40 mM $MgCl_2$ solution (Supplementary Figure 3). Oocytes were impaled with electrodes filled with 3 M KCl. Changes in junction potentials after bath perfusion ranged from -0.2 mV to -2.0 mV. Error bars indicate standard error of the mean. All experiments were performed at room temperature.

Relative permeability ratios were calculated as previously reported (Fatt and Ginsborg, 1958; Schmidt and Schroeder, 1994). Experiments were analyzed in environments in which Ca^{2+} or Mg^{2+} were the only permeable cations in the bath solution and the intracellular K^+ concentration was valued at 100 mM (Schroeder et al., 1994).

Mesophyll protoplast transformation and confocal microscopy

Arabidopsis mesophyll protoplasts were transformed following a published procedure (Sheen, 2002). Protoplasts were incubated at 20˚C in the dark for at least 16 hours before microscopy analysis. For FM4-64 protoplast staining, the dye was directly added to the suspension at a final concentration of 17 µM (Horie et al., 2007). Fluorescence microscopy analyses were carried out after five minutes of incubation.

Confocal microscope analyses were performed using a Nikon PCM2000 (Bio-Rad, Germany) laser scanning confocal imaging system. For GFP detection, excitation was at 488 nm and detection between 515 and 530 nm. For the chlorophyll and FM4-64 detection, excitation was at 488 nm and detection over 570 nm. The images acquired from the confocal microscope were processed using ImageJ (http://rsbweb.nih.gov/ij/).

Acknowledgements

We thank Dr. Rodríguez-Navarro (Universidad Politécnica de Madrid, Spain) for providing us with *OsHKT2;3* and *OsHKT2;4* cDNAs and Takayuki Sasaki (IPSR, Okayama Univ., Japan) for helpful discussion.

Figure captions

Figure 1. OsHKT2;4 complements high-affinity K^+ uptake deficient mutant *S. cerevisiae* strain CY162. CY162 cells were transformed with an empty vector pYES2 and members of the *Oryza sativa* HKT family, OsHKT2;1, OsHKT2;2, OsHKT2;3 and OsHKT2;4. Growth was monitored on arginine phosphate (AP) medium. (A) Growth of each CY162 transformant on AP medium supplemented with 10 mM KCl, incubated at 30°C for 2 days. (B) Growth of each CY162 transformant on AP medium supplemented with 0.1 mM KCl, incubated at 30°C for 4 days. Three independent clones were tested for every condition with similar results.

Figure 2. OsHKT2;4 reduces salt sensitivity in growth inhibition tests using the Na^+ hypersensitive mutant strain of *S. cerevisiae*, G19 in which all four ENA Na^+ ATPases were

deleted (MATa, *his3*, *ura3*, *trp1*, *ade2*, and *ena1::HIS3::ena4*). G19 yeast cells were transformed with an empty vector pYES2 and the indicated OsHKT transporters described in Figure 1. Growth was monitored on arginine phosphate (AP) medium. (A) Growth of each G19 transformant on AP medium supplemented with 1 mM KCl and either (A) 50 mM NaCl; (B) 100 mM NaCl; (C) 150 mM NaCl; or (D) 200 mM NaCl. Expression of the K^+-uptake-mediating OsHKT2;4 (Fig. 1) and OsHKT2;2 transporters reduced salt sensitivity. As expected, the Na^+ influx transporter OsHKT2;1 enhanced Na^+ sensitivity under all conditions. G19 cells were grown at 30°C for 10 days. Three independent clones were tested for every condition with similar results.

Figure 3. OsHKT2;4 expression in *X. laevis* oocytes mediates inward ion currents for all five alkali cations analyzed. (A) The current-voltage relationships from oocytes injected with 50 ng of *OsHKT2;4* cRNA are shown. Oocytes were bathed in solutions supplemented with 10 mM alkali monovalent cations as chloride salts. Note that only background currents of water-injected control oocytes bathed in a 10 mM NaCl solution are presented as a representative control, as no significant differences were found among the five ionic conditions in controls. Currents were recorded from a holding potential of -40 mV using a step command with 15-mV decrements as described in Yao et al., 2010 (see also "Materials and Methods"). Error bars represent ± SE (n = 5 for water injected control and n = 6 for OsHKT2;4-expressing oocytes at each condition). (B) Amplitudes of OsHKT2-mediated inward currents, recorded at -150 mV. Voltage clamp experiments were performed in the presence of 10 mM NaCl. Note that data for OsHKT2;4-expressing and water-injected oocytes are the same as the recordings presented in A, and 12.5 ng of cRNA was injected into oocytes for the recordings of OsHKT2;1- and OsHKT2;2-mediated currents. Error bars represent ± SE (n = 5 for water-injected control and n = 6 for OsHKT2-expressing oocytes).

Figure 4. OsHKT2;4 exhibits robust K^+ but weak Na^+ permeability. Current-voltage relationships from oocytes injected with 50 ng of *OsHKT2;4* cRNA are shown. (A) OsHKT2;4-expressing oocytes were bathed in a 0.3 mM Na^+ solution supplemented with the indicated concentrations of K^+. (B) OsHKT2;4-expressing oocytes were bathed in a 0.3 mM K^+ solution supplemented with the indicated concentrations of Na^+. (A-B) Currents were recorded from a

holding voltage of -40 mV using step commands with 15-mV decrements. Note that only the background currents of water-injected control oocytes bathed in a 0.3 mM Na^+ & 10 mM K^+ solution (A) or a 0.3 mM K^+ & 10 mM Na^+ solution (B) were presented as representative controls as no significant difference was found among the ionic conditions tested. Error bars represent ± SE (n = 5 for water injected control and n = 12-13 for OsHKT2;4-expressing oocytes at each condition). K^+ and Na^+ were added to the bath solutions as glutamate salts.

Figure 5. OsHKT2;4-mediated K^+-dependent growth is less sensitive to high concentrations of Na^+ compared to OsHKT2;2. CY162 cells harboring pYES2 or cells expressing OsHKT2;2 or OsHKT2;4 were grown on arginine phosphate (AP) medium containing the indicated concentrations of K^+ and Na^+. (A) Growth of each CY162 transformant on AP medium supplemented with 0.1 mM KCl and the indicated concentrations of NaCl. (B) Growth of each CY162 transformant on AP medium supplemented with 1.0 mM KCl and indicated amount of NaCl. Each transformant was pre-cultured in liquid SC-Ura + 50 mM KCl medium and 1:10 serial dilutions in AP medium with no added K^+ and Na^+ were spotted on plates. All plates were incubated at 30°C for 6 days and photographs were taken afterwards.

Figure 6. OsHKT2;4 mediates inward K^+ currents in the absence of extracellularly added Na^+ in *X. laevis* oocytes. Current-voltage relationships from oocytes injected with 50 ng of *OsHKT2;4* cRNA are shown. During OsHKT2;4-mediated current recordings, the K^+ concentration of the bath solution was increased from 0.3 mM to 10 mM. Note that only the background currents of water-injected control oocytes bathed in a 10 mM K^+ solution were presented as a representative control as no significant difference was found among the three ionic conditions. Currents were recorded from a holding voltage of -40 mV using step commands with 15-mV decrements and error bars represent ± SE (n = 6 for each condition). K^+ was added to the bath solutions as a glutamate salt.

Figure 7. OsHKT2;4 mediates K^+ uptake in yeast cells. (A) CY162 cells harboring pYES2 or the cells expressing OsHKT2;2 or OsHKT2;4 were grown on arginine phosphate (AP) medium supplemented with the indicated concentrations of KCl. Each transformant was pre-cultured in liquid SC-Ura + 50 mM KCl medium and 1:10 serial dilutions in AP medium with no added K^+

and Na^+ were spotted on plates. All plates were incubated at 30°C for 6 days and photographs were taken afterwards. (B) Concentration-dependent increases in the growth rate of OsHKT2;4-expressing CY162 cells. CY162 cells harboring pYES2 or pYES2::*OsHKT2;4* cDNA were inoculated into liquid AP medium supplemented with either 0.025, 0.05, 0.075, 0.1, 0.25, 0.5 or 1.0 mM KCl at a starting OD_{600} of 0.01. Growth of the cells was monitored and the slopes from the linear regression to the growth curves at the logarithmic growth phase of OsHKT2;4-expressing cells were obtained and plotted. The curve in the graph was obtained by a non-linear regression analysis using the Michaelis-Menten curve fitting formula. Three independent experiments were performed and error bars represent ± SD.

Figure 8. Five HKT family transporters were tested for Mg^{2+} and Ca^{2+} permeability in the presence of 5 mM and 50 mM extracellular concentrations of $MgCl_2$ or $CaCl_2$. AtHKT1;1 and OsHKT2;1 (A,B) showed small changes in the reversal potentials of HKT-mediated currents, even upon extracellular exposure to high 50 mM concentrations of these divalent cations. OsHKT2;2 (C) showed a moderate +13 mV reversal potential shift upon increasing Mg^{2+} from 5 to 50 mM, but the observed current magnitudes were unchanged. OsHKT2;4 and TaHKT2;1 (D,E) exhibited notable shifts in the reversal potentials in response to 50 mM Mg^{2+} concentrations. OsHKT2;4 showed a +33 mV reversal potential shift upon increasing $MgCl_2$ concentration from 5 to 50 mM, and a +45 mV shift for $CaCl_2$ upon increasing concentration from 5 to 50 mM. TaHKT2;1 showed a +20 mV shift for $MgCl_2$ after increasing the bath concentration from 5 to 50 mM, and a -2 mV shift for a 5 to 50 mM $CaCl_2$ increase. Currents were recorded from a holding voltage of -40 mV using a 2.5-second ramp protocol ranging from 0 mV to -150 mV. Specific data points from voltage ramps at -150 mV, -100 mV, -50 mV, and 0 mV were analyzed for the current-voltage graphs, which were used to determine reversal potentials. Error bars represent ± SE (n = 6-53, depending on condition and transporter tested).

Figure 9. OsHKT2;4 mediates Ca^{2+} and Mg^{2+} transport. The addition of 50 mM Ca^{2+} or Mg^{2+} resulted in large, time dependent inward cation currents for (B) OsHKT2;4 compared to controls (A). (A) Small currents were detected in water-injected control oocytes. A bath solution containing 50 mM $CaCl_2$ was used for the control recording shown. (B) Similar current magnitudes were observed for the 50 mM Ca^{2+} and Mg^{2+} groups in OsHKT2;4. Slow time-

dependent activation was commonly observed in OsHKT2;4-injected oocytes during hyperpolarized voltages. (C) Currents recorded in TaHKT2;1-expressing oocytes at the indicated $MgCl_2$ and $CaCl_2$ concentrations. Unlike in OsHKT2;4, slow time-dependent deactivation was commonly observed in TaHKT2;1-injected oocytes during hyperpolarized voltages. Zero current levels are shown by arrows on the left of the recorded currents. Voltage steps ranged from -150 mV to +60 mV in 30 mV increments. The final "tail" voltage at the end of the pulses was +40 mV.

Figure 10. Inhibition of strong Mg^{2+} and Ca^{2+} permeabilities in OsHKT2;4 and TaHKT2;1 was observed in the presence of competing K^+ and Na^+ ions. (A) OsHKT2;4 was analyzed for relative Mg^{2+} and Ca^{2+} permeabilities in the presence of 10 mM K^+. (B) TaHKT2;1 was analyzed for relative Mg^{2+} and Ca^{2+} permeabilities in the presence of 10 mM Na^+ and 3 mM K^+. (A) OsHKT2;4 showed a +5 mV reversal potential shift upon adding 50 mM $MgCl_2$ to the 10 mM KCl competition control solution. Addition of $CaCl_2$ also resulted in a small average +4 mV reversal potential shift. (B) TaHKT2;1 exhibited a +6 mV reversal potential shift upon adding 50 mM $MgCl_2$ to the 10 mM NaCl, 3 mM KCl control solution. Addition of 50 mM $CaCl_2$ to the control solution resulted in a smaller +3 mV reversal potential shift. (C) K^+ permeability was observed in the presence of competing Ca^{2+} ions. OsHKT2;4 showed a -2 mV reversal potential shift upon addition of 0.1 mM K^+ to the 5 mM Ca^{2+} bath solution, a +16 mV reversal shift upon addition of 1 mM K^+, and a +36 mV reversal shift upon addition of 10 mM K^+ to the bath solution. Currents were recorded from a holding voltage of -40 mV using step commands with 30-mV decrements and error bars represent ± SE (n = 12-19, depending on condition and transporter tested).

Figure 11. Subcellular localization of EGFP-OsHKT2;4 in *Arabidopsis* mesophyll protoplasts. EGFP-OsHKT2;4 protein was transiently expressed in protoplasts of *Arabidopsis* mesophyll cells under the control of the CaMV 35S promoter. Fluorescence was analyzed by confocal microscopy. (A) EGFP fluorescence (green) from the chimeric EGFP-OsHKT2;4 protein shows fluorescence at the periphery of the protoplast. (B) Chlorophyll auto fluorescence (red) of the same protoplast shown in (A). (C) Overlay image of (A) and (B). (D) Control EGFP fluorescence (green) from the free EGFP. (E) Chlorophyll auto fluorescence (red) of the same protoplast

shown in (D). (F) Overlay image of (E) and (D). (G) Confocal EGFP fluorescence (green) image from a focal plane of an EGFP-OsHKT2;4-expressing cell. (H) FM4-64 fluorescence image of the same protoplast shown in (G). (I) Overlay image of (G) and (H). (J) Confocal EGFP fluorescence (green) image of an EGFP-expressing cell. (K) FM4-64 fluorescence image of the same protoplast shown in (J). (L) Overlay image of (J) and (K).

Literature cited

Almers W, McCleskey EW, Palade PT (1984) A non-selective cation conductance in frog muscle membrane blocked by micromolar external calcium ions. J Physiol. **353:** 565-583

Anderson JA, Huprikar SS, Kochian LV, Lucas WJ, Gaber RF (1992) Functional expression of a probable *Arabidopsis thaliana* potassium channel in *Saccharomyces cerevisiae*. Proc Natl Acad Sci U S A. **89:** 3736-3740

Barish ME (1983) A transient calcium-dependent chloride current in the immature *Xenopus* oocyte. J Physiol. **342:** 309-325

Berthomieu P, Conejero G, Nublat A, Brackenbury W, Lambert C, Savio C, Uozumi N, Oiki S, Yamada K, Cellier F, Gosti F, Simonneau T, Essah P, Tester M, Very A, Sentenac H, Casse F (2003) Functional analysis of AtHKT1 in *Arabidopsis* shows that Na^+ recirculation by the phloem is crucial for salt tolerance. EMBO J. **22:** 2004-2014

Bolte S, Talbot C, Boutte Y, Catrice O, Read ND, Satiat-Jeunemaitre B (2004) FM-dyes as experimental probes for dissecting vesicle trafficking in living plant cells. J Microsc. **214:** 159-173

Byrt CS, Platten JD, Spielmeyer W, James RA, Lagudah ES, Dennis ES, Tester M, Munns R (2007) HKT1;5-like cation transporters linked to Na^+ exclusion loci in wheat, *Nax2* and *Kna1*. Plant Physiol. **143:** 1918-1928

Cao Y, Crawford NM, Schroeder JI (1995) Amino terminus and the first four membrane-spanning segments of the *Arabidopsis* K^+ channel KAT1 confer inward-rectification property of plant-animal chimeric channels. J Biol Chem. **270:** 17697-17701

Cao Y, Jin X, Huang H, Derebe MG, Levin EJ, Kabaleeswaran V, Pan Y, Punta M, Love J, Weng J, Quick M, Ye S, Kloss B, Bruni R, Martinez-Hackert E, Hendrickson WA, Rost B, Javitch JA, Rajashankar KR, Jiang Y, Zhou M (2011) Crystal structure of a potassium ion transporter, TrkH. Nature **471:** 336-340

Corratgé C, Zimmermann S, Lambilliotte R, Plassard C, Marmeisse R, Thibaud JB, Lacombe B, Sentenac H (2007) Molecular and functional characterization of a Na^+-K^+ transporter from the Trk family in the ectomycorrhizal fungus *Hebeloma cylindrosporum*. J Biol Chem. **282:** 26057-26066

Davenport RJ, Munoz-Mayor A, Jha D, Essah PA, Rus A, Tester M (2007) The Na^+ transporter AtHKT1;1 controls retrieval of Na+ from the xylem in Arabidopsis. Plant Cell Environ. **30:** 497-507

Doyle DA, Morais Cabral J, Pfuetzner RA, Kuo A, Gulbis JM, Cohen SL, Chait BT, MacKinnon R (1998) The structure of the potassium channel: molecular basis of K^+ conduction and selectivity. Science. **280:** 69-77

Durell SR, Guy HR (1999) Structural models of the KtrB, TrkH, and Trk1,2 symporters based

on the structure of the KcsA K^+ channel. Biophys J. **77:** 789-807

Durell SR, Hao Y, Nakamura T, Bakker EP, Guy HR (1999) Evolutionary relationship between K^+ channels and symporters. Biophys J. **77:** 775-788

Fatt P, Ginsborg BL (1958) The ionic requirements for the production of action potentials in crustacean muscle fibres. J Physiol. **142:** 516-543

Flowers TJ, Läuchli A (1983) Sodium versus potassium: Substitution and compartmentation. Inorganic plant nutrition **15b:** 651-681

Fu H-H, Luan S (1998) AtKUP1: A Dual-Affinity K+ Transporter from Arabidopsis. The Plant Cell **10:** 63-74

Garciadeblás B, Senn M, Banuelos M, Rodriguez-Navarro A (2003) Sodium transport and HKT transporters: the rice model. Plant J. **34:** 788-801

Gassmann W, Rubio F, Schroeder JI (1996) Alkali cation selectivity of the wheat root high-affinity potassium transporter HKT1. Plant J. **10:** 869-882

Gierth M, Mäser P (2007) Potassium transporters in plants--involvement in K^+ acquisition, redistribution and homeostasis. FEBS Lett. **581:** 2348-2356

Gierth M, Mäser P, Schroeder JI (2005) The Potassium Transporter AtHAK5 Functions in K+ Deprivation-Induced High-Affinity K+ Uptake and AKT1 K+ Channel Contribution to K+ Uptake Kinetics in Arabidopsis Roots. Plant Physiology **137:** 1105-1114

Glass ADM (1983) Regulation of Ion Transport. Ann Rev Plant Physiol. **34:** 311-326

Golldack D, Su H, Quigley F, Kamasani UR, Muñz-Garay C, Balderas E, Popova OV, Bennett J, Bohnert HJ, Pantoja O (2002) Characterization of a HKT-type transporter in rice as a general alkali cation transporter. Plant J. **34:** 1-14

Hauser F, Horie T (2010) A conserved primary salt tolerance mechanism mediated by HKT transporters: a mechanism for sodium exclusion and maintenance of high K/Na ratio in leaves during salinity stress. Plant Cell Environ. **33:** 552-565

Hille B (1992) Ionic Channels of Excitable Membranes 2nd Edition. Sinauer Associates Inc.,Sunderland, Massachusetts

Hirochika H, Sugimoto K, Otsuki Y, Tsugawa H, Kanda M (1996) Retrotransposons of rice involved in mutations induced by tissue culture. Proc Natl Acad Sci U S A. **93:** 7783-7788

Horie T, Costa A, Kim TH, Han MJ, Horie R, Leung HY, Miyao A, Hirochika H, An G, Schroeder JI (2007) Rice OsHKT2;1 transporter mediates large Na^+ influx component into K^+-starved roots for growth. EMBO J. **26:** 3003-3014

Horie T, Hauser F, Schroeder JI (2009) HKT transporter-mediated salinity resistance mechanisms in *Arabidopsis* and monocot crop plants. Trends Plant Sci. **14:** 660-668

Horie T, Horie R, Chan WY, Leung HY, Schroeder JI (2006) Calcium regulation of sodium hypersensitivities of *sos3* and *athkt1* mutants. Plant Cell Physiol. **47:** 622-633

Horie T, Yoshida K, Nakayama H, Yamada K, Oiki S, Shinmyo A (2001) Two types of HKT transporters with different properties of Na^+ and K^+ transport in *Oryza sativa*. Plant J. **27:** 129-138

Huang S, Spielmeyer W, Lagudah ES, James RA, Platten JD, Dennis ES, Munns R (2006) A sodium transporter (HKT7) is a candidate for *Nax1*, a gene for salt tolerance in durum wheat. Plant Physiol. **142:** 1718-1727

Huang S, Spielmeyer W, Lagudah ES, Munns R (2008) Comparative mapping of HKT genes in wheat, barley, and rice, key determinants of Na^+ transport, and salt tolerance. J Exp Bot. **59:** 927-937

Jabnoune M, Espeout S, Mieulet D, Fizames C, Verdeil JL, Conejero G, Rodriguez-Navarro A, Sentenac H, Guiderdoni E, Abdelly C, Very AA (2009) Diversity in expression patterns and functional properties in the rice HKT transporter family. Plant Physiol. **150:** 1955-1971

Kim EJ, Kwak JM, Uozumi N, Schroeder JI (1998) AtKUP1: An Arabidopsis Gene Encoding High-Affinity Potassium Transport Activity. The Plant Cell **10:** 51-62

Kwak JM, Murata Y, Baizabal-Aguirre VM, Merrill J, Wang M, Kemper A, Hawke SD, Tallman G, Schroeder JI (2001) Dominant negative guard cell K^+ channel mutants reduce inward-rectifying K^+ currents and light-induced stomatal opening in *Arabidopsis*. Plant Physiol. **127:** 473-485

Lacombe B, Becker D, Hedrich R, DeSalle R, Hollmann M, Kwak JM, Schroeder JI, Le Novere N, Nam HG, Spalding EP, Tester M, Turano FJ, Chiu J, Coruzzi G (2001) The identity of plant glutamate receptors. Science **292:** 1486-1487

Lan WZ, Wang W, Wang SM, Li LG, Buchanan BB, Lin HX, Gao JP, Luan S (2010) A rice high-affinity potassium transporter (HKT) conceals a calcium-permeable cation channel. Proc Natl Acad Sci U S A. **107:** 7089-7094

Laurie S, Feeney KA, Maathuis FJM, Heard PJ, Brown SJ, Leigh RA (2002) A role for HKT1 in sodium uptake by wheat roots. Plant J. **32:** 139-149

Lebaudy A, Very AA, Sentenac H (2007) K^+ channel activity in plants: genes, regulations and functions. FEBS Lett. **581:** 2357-2366

Liu W, Fairbairn DJ, Reid RJ, Schachtman DP (2001) Characterization of two HKT1 homologues from *Eucalyptus camaldulensis* that display intrinsic osmosensing capability. Plant Physiol. **127:** 283-294

Liu W, Schachtman DP, Zhang W (2000) Partial Deletion of a Loop Region in the High Affinity K+ Transporter HKT1 Changes Ionic Permeability Leading to Increased Salt Tolerance. Journal of Biological Chemistry **275:** 27924-27932

Mäser P, Eckelman B, Vaidyanathan R, Horie T, Fairbairn D, Kubo M, Yamagami M, Yamaguchi K, Nishimura M, Uozumi N, Robertson W, Sussman MR, Schroeder JI (2002a) Altered shoot/root Na^+ distribution and bifurcating salt sensitivity in *Arabidopsis* by genetic disruption of the Na^+ transporter AtHKT1. FEBS Lett **531:** 157-161

Mäser P, Hosoo Y, Goshima S, Horie T, Eckelman B, Yamada K, Yoshida K, Bakker EP, Shinmyo A, Oiki S, Schroeder JI, Uozumi N (2002b) Glycine residues in potassium channel-like selectivity filters determine potassium selectivity in four-loop-per-subunit HKT transporters from plants. Proc Natl Acad Sci U S A. **99:** 6428-6433

Miyao A, Tanaka K, Murata K, Sawaki H, Takeda S, Abe K, Shinozuka Y, Onosato K, Hirochika H (2003) Target site specificity of the *Tos17* retrotransposon shows a preference for insertion within genes and against insertion in retrotransposon-rich regions of the genome. Plant Cell. **15:** 1771-1780

Møller IS, Gilliham M, Jha D, Mayo GM, Roy SJ, Coates JC, Haseloff J, Tester M (2009) Shoot Na^+ exclusion and increased salinity tolerance engineered by cell type-specific alteration of Na^+ transport in *Arabidopsis*. Plant Cell **21:** 2163-2178

Platten JD, Cotsaftis O, Berthomieu P, Bohnert H, Davenport RJ, Fairbairn DJ, Horie T, Leigh RA, Lin HX, Luan S, Mäser P, Pantoja O, Rodriguez-Navarro A, Schachtman DP, Schroeder JI, Sentenac H, Uozumi N, Very AA, Zhu JK, Dennis ES, Tester M (2006) Nomenclature for HKT transporters, key determinants of plant salinity tolerance. Trends in Plant Science **11:** 372-374

Preston GM, Carroll TP, Guggino WB, Agre P (1992) Appearance of water channels in *Xenopus oocytes* expressing red cell CHIP28 protein. Science. **256:** 385-387

Pyo YJ, Gierth M, Schroeder JI, Cho MH (2010) High-Affinity K^+ Transport in Arabidopsis: AtHAK5 and AKT1 Are Vital for Seedling Establishment and Postgermination Growth under Low-Potassium Conditions. Plant Physiology **153:** 863-875

Quintero FJ, Blatt MR (1997) A new family of K+ transporters from Arabidopsis that are conserved across phyla. FEBS Letters **415:** 206-211

Quintero FJ, Garciadeblas B, Rodriguez-Navarro A (1996) The *SAL1* gene of Arabidopsis, encoding an enzyme with 3'(2'),5'-bisphosphate nucleotidase and inositol polyphosphate 1-phosphatase activities, increases salt tolerance in yeast. The Plant Cell **8:** 529-537

Ren ZH, Gao JP, Li LG, Cai XL, Huang W, Chao DY, Zhu MZ, Wang ZY, Luan S, Lin HX (2005) A rice quantitative trait locus for salt tolerance encodes a sodium transporter. Nat Genet. **37:** 1141-1146

Rodríguez-Navarro A, Ramos J (1984) Dual system for potassium transport in *Saccharomyces cerevisiae*. J Bacteriol. **159:** 940-945

Rubio F, Gassmann W, Schroeder JI (1995) Sodium-Driven Potassium Uptake by the Plant Potassium Transporter HKT1 and Mutations Conferring Salt Tolerance. Science **270:** 1660-1663

Rubio F, Schwarz M, Gassmann W, Schroeder JI (1999) Genetic Selection of Mutations in the High Affinity K+ Transporter HKT1 That Define Functions of a Loop Site for Reduced Na+ Permeability and Increased Na+Tolerance. Journal of Biological Chemistry **274:** 6839-6847

Santa-Maria GE, Rubio F, Dubcovsky J, Rodriguez-Navarro A (1997) The HAK1 Gene of Barley Is a Member of a Large Gene Family and Encodes a High-Affinity Potassium Transporter. The Plant Cell **9:** 2281-2289

Schachtman DP, Schroeder JI (1994) Structure and transport mechanism of a high-affinity potassium uptake transporter from higher plants. Nature. **370:** 655-658

Schmidt C, Schroeder JI (1994) Anion selectivity of slow anion channels in the plasma membrane of guard cells (large nitrate permeability). Plant Physiol. **106:** 383-391

Schroeder JI (1989) Quantitative analysis of outward rectifying K^+ channel currents in guard cell protoplasts from *Vicia faba*. J Membr Biol. **107:** 229-235

Schroeder JI, Ward JM, Gassmann W (1994) Perspectives on the Physiology and Structure of Inward-Rectifying K^+ Channels in Higher-Plants - Biophysical Implications for K^+ Uptake. Annu Rev Biophys Biomol Struct. **23:** 441-471

Sheen J (2002) A transient expression assay using *Arabidopsis* mesophyll protoplasts. http://genetics.mgh.harvard.edu/sheenweb/

Sunarpi, Horie T, Motoda J, Kubo M, Yang H, Yoda K, Horie R, Chan WY, Leung HY, Hattori K, Konomi M, Osumi M, Yamagami M, Schroeder JI, Uozumi N (2005) Enhanced salt tolerance mediated by AtHKT1 transporter-induced Na^+ unloading from xylem vessels to xylem parenchyma cells. Plant J. **44:** 928-938

Takahashi R, Liu S, Takano T (2007) Cloning and functional comparison of a high-affinity K+ transporter gene PhaHKT1 of salt-tolerant and salt-sensitive reed plants. Journal of Experimental Botany **58:** 4387-4395

Tholema N, Vor der Bruggen M, Mäser P, Nakamura T, Schroeder JI, Kobayashi H, Uozumi N, Bakker EP (2005) All four putative selectivity filter glycine residues in KtrB are essential for high affinity and selective K^+ uptake by the KtrAB system from *Vibrio*

alginolyticus. J Biol Chem. **280:** 41146-41154

Uozumi N, Gassmann W, Cao Y, Schroeder JI (1995) Identification of strong modifications in cation selectivity in an *Arabidopsis* inward rectifying potassium channel by mutant selection in yeast. J Biol Chem. **270:** 24276-24281

Uozumi N, Kim EJ, Rubio F, Yamaguchi T, Muto S, Tsuboi A, Bakker EP, Nakamura T, Schroeder JI (2000) The *Arabidopsis HKT1* gene homolog mediates inward Na^+ currents in *Xenopus laevis* oocytes and Na^+ uptake in *Saccharomyces cerevisiae*. Plant Physiol. **122:** 1249-1259

Véry AA, Sentenac H (2003) Molecular mechanisms and regulation of K^+ transport in higher plants. Annu Rev Plant Biol. **54:** 575-603

Walker DJ, Black CR, Miller AJ (1998) The role of cytosolic potassium and pH in the growth of barley roots. Plant Physiol. **118:** 957-964

Walker DJ, Leigh RA, Miller AJ (1996) Potassium homeostasis in vacuolate plant cells. Proc Natl Acad Sci U S A. **93:** 10510-10514

Wang TB, Gassmann W, Rubio F, Schroeder JI, Glass ADM (1998) Rapid up-regulation of *HKT1*, a high-affinity potassium transporter gene, in roots of barley and wheat following withdrawal of potassium. Plant Physiol. **118:** 651-659

Ward JM, Mäser P, Schroeder JI (2009) Plant ion channels: gene families, physiology, and functional genomics analyses. Annu Rev Physiol. **71:** 59-82

Yao X, Horie T, Xue S, Leung H-Y, Katsuhara M, Brodsky DE, Wu Y, Schroeder JI (2010) Differential Sodium and Potassium Transport Selectivities of the Rice OsHKT2;1 and OsHKT2;2 Transporters in Plant Cells. Plant Physiology **152:** 341-355

Yenush L, Mulet JM, Arino J, Serrano R (2002) The Ppz protein phosphatases are key regulators of K^+ and pH homeostasis: implications for salt tolerance, cell wall integrity and cell cycle progression. EMBO J. **21:** 920-929

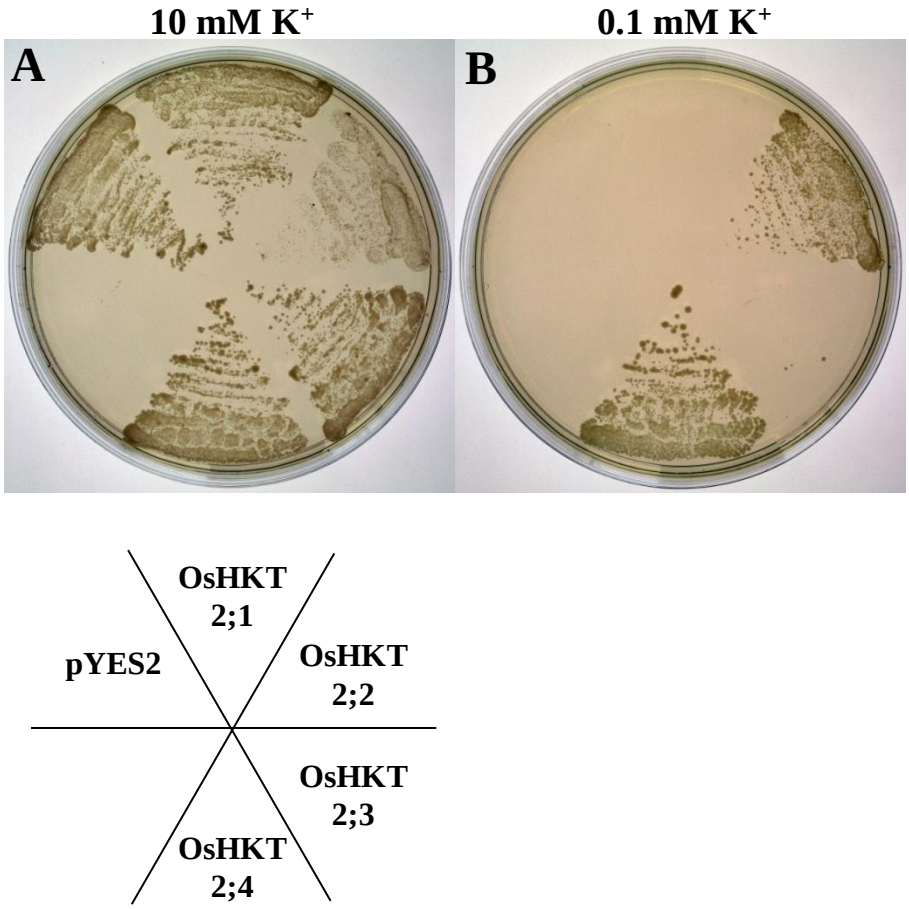

Figure 1. OsHKT2;4 complements high-affinity K^+ uptake deficient mutant *S. cerevisiae* strain CY162. CY162 cells were transformed with an empty vector pYES2 and members of the *Oryza Sativa* HKT family, OsHKT2;1, OsHKT2;2, OsHKT2;3 and OsHKT2;4. Growth was monitored on arginine phosphate (AP) medium. (A) Growth of each CY162 transformant on AP medium supplemented with 10 mM KCl, incubated at 30° C for 2 days. (B) Growth of each CY162 transformant on AP medium supplemented with 0.1 mM KCl, incubated at 30° C for 4 days. Three independent clones were tested for every condition with similar results.

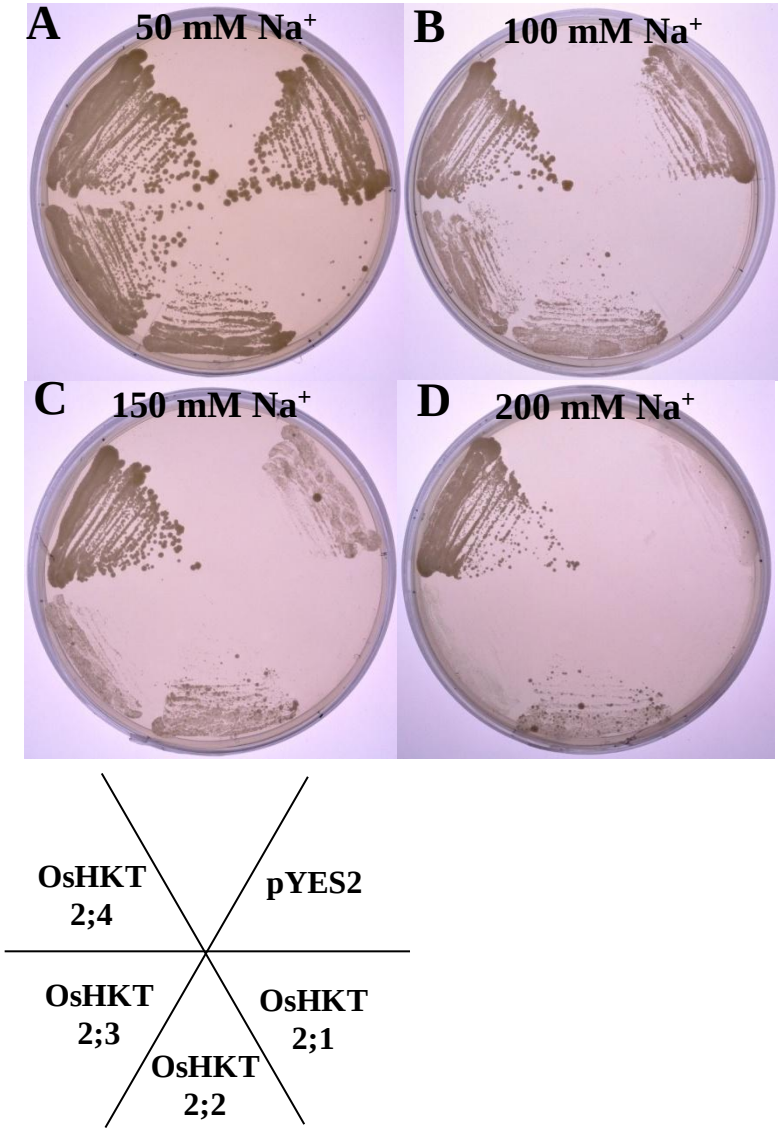

Figure 2. OsHKT2;4 reduces salt sensitivity in growth inhibition tests using the Na^+ hypersensitive mutant strain of *S. cerevisiae*, G19 in which all four ENA Na^+ ATPases were deleted (MATa, *his3*, *ura3*, *trp1*, *ade2*, and *ena1::HIS3::ena4*). G19 yeast cells were transformed with an empty vector pYES2 and the indicated OsHKT transporters described in Figure 1. Growth was monitored on arginine phosphate (AP) medium. (A) Growth of each G19 transformant on AP medium supplemented with 1 mM KCl and either (A) 50 mM NaCl; (B) 100 mM NaCl; (C) 150 mM NaCl; or (D) 200 mM NaCl. Expression of the K^+-uptake-mediating OsHKT2;4 (Fig. 1) and OsHKT2;2 transporters reduced salt sensitivity. As expected, the Na^+ influx transporter OsHKT2;1 enhanced Na^+ sensitivity under all conditions. G19 cells were grown at 30° C for 10 days. Three independent clones were tested for every condition with similar results.

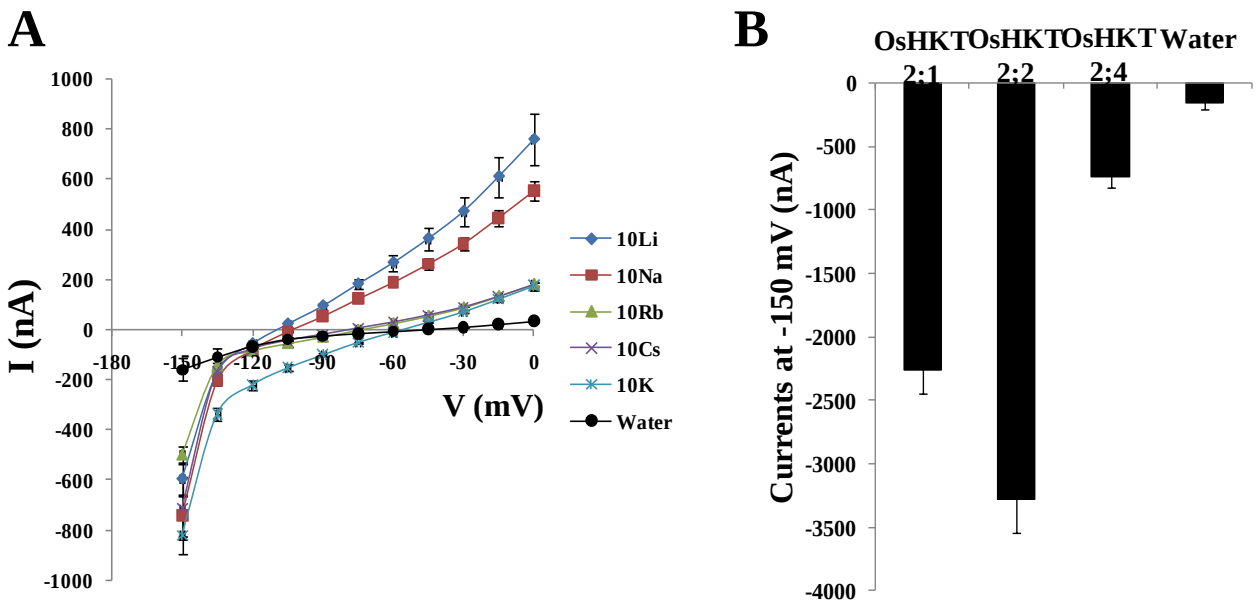

Figure 3. OsHKT2;4 expression in *X. laevis* oocytes mediates inward ion currents for all five alkali cations analyzed. (A) The current-voltage relationships from oocytes injected with 50 ng of *OsHKT2;4* cRNA are shown. Oocytes were bathed in solutions supplemented with 10 mM alkali monovalent cations as chloride salts. Note that only background currents of water-injected control oocytes bathed in a 10 mM NaCl solution are presented as a representative control, as no significant differences were found among the five ionic conditions in controls. Currents were recorded from a holding potential of -40 mV using a step command with 15-mV decrements as described in Yao et al. (2010) (see also "Materials and Methods"). Error bars represent ± SE (n = 5 for water injected control and n = 6 for OsHKT2;4-expressing oocytes at each condition). (B) Amplitudes of OsHKT2-mediated inward currents, recorded at -150 mV. Voltage clamp experiments were performed in the presence of 10 mM NaCl. Note that data for OsHKT2;4-expressing and water-injected oocytes are the same as the recordings presented in A, and 12.5 ng of cRNA was injected into oocytes for the recordings of OsHKT2;1- and OsHKT2;2-mediated currents. Error bars represent ± SE (n = 5 for water injected control and n = 6 for OsHKT2-expressing oocytes).

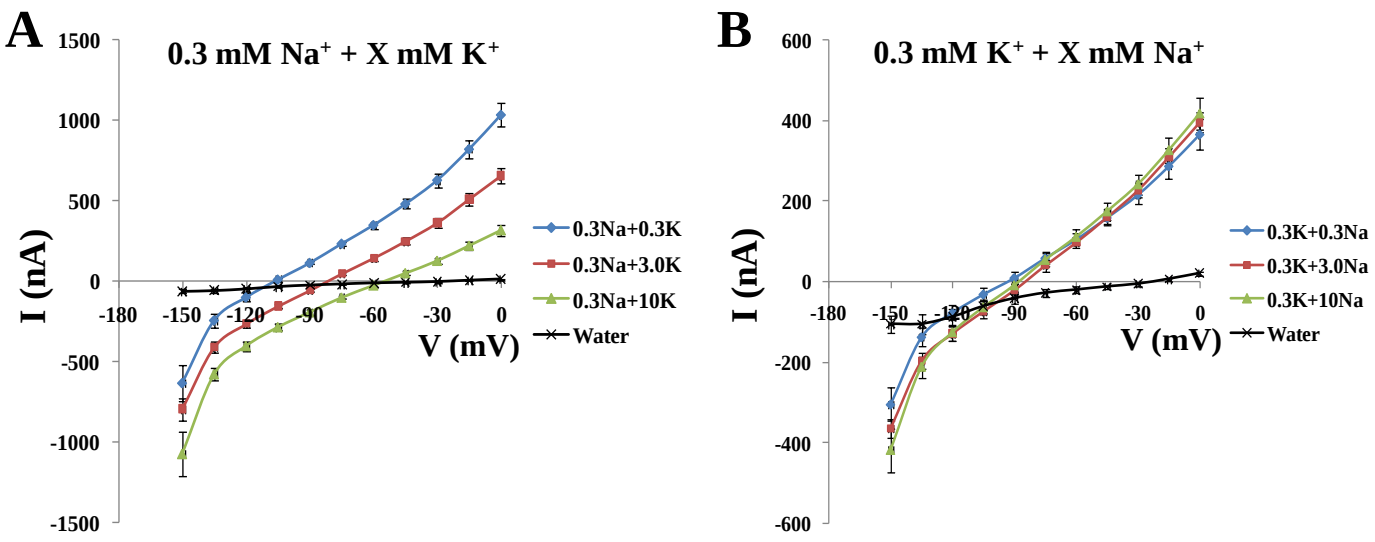

Figure 4. OsHKT2;4 exhibits robust K^+ but weak Na^+ permeability. Current-voltage relationships from oocytes injected with 50 ng of *OsHKT2;4* cRNA are shown. (A) OsHKT2;4-expressing oocytes were bathed in a 0.3 mM Na^+ solution supplemented with the indicated concentrations of K^+. (B) OsHKT2;4-expressing oocytes were bathed in a 0.3 mM K^+ solution supplemented with the indicated concentrations of Na^+. (A-B) Currents were recorded from a holding voltage of -40 mV using step commands with 15-mV decrements. Note that only the background currents of water-injected control oocytes bathed in a 0.3 mM Na^+ & 10 mM K^+ solution (A) or a 0.3 mM K^+ & 10 mM Na^+ solution (B) were presented as representative controls as no significant difference was found among the ionic conditions tested. Error bars represent ± SE (n = 5 for water injected control and n = 12-13 for OsHKT2;4-expressing oocytes at each condition). K^+ and Na^+ were added to the bath solutions as glutamate salts.

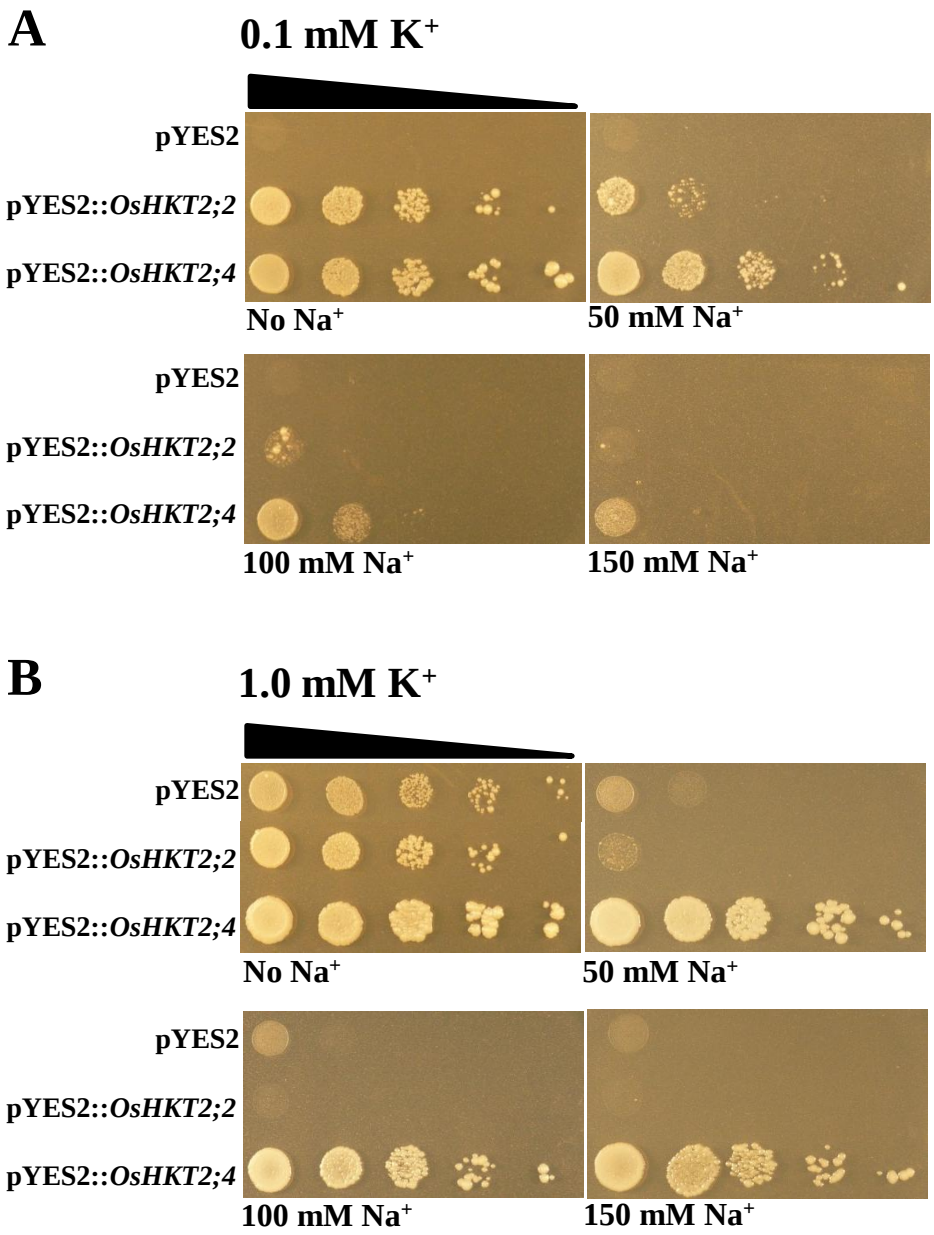

Figure 5. OsHKT2;4-mediated K^+-dependent growth is less sensitive to high concentrations of Na^+ compared to OsHKT2;2. CY162 cells harboring pYES2 or cells expressing OsHKT2;2 or OsHKT2;4 were grown on arginine phosphate (AP) medium containing the indicated concentrations of K^+ and Na^+. (A) Growth of each CY162 transformant on AP medium supplemented with 0.1 mM KCl and the indicated concentrations of NaCl. (B) Growth of each CY162 transformant on AP medium supplemented with 1.0 mM KCl and indicated amount of NaCl. Each transformant was grown in liquid SC-Ura + 50 mM KCl medium and 1:10 serial dilutions were spotted on plates. All plates were incubated at 30° C for 6 days and photographs were taken afterwards.

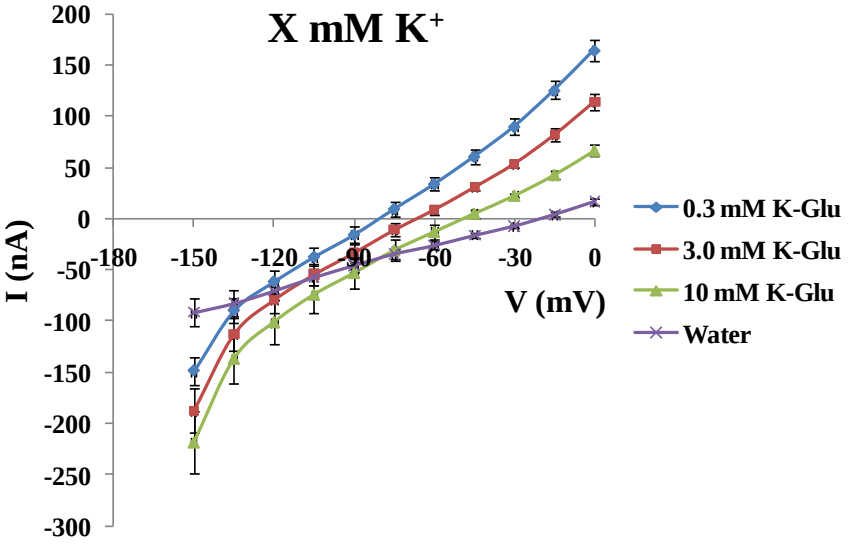

Figure 6. OsHKT2;4 mediates inward K^+ currents in the absence of extracellularly added Na^+ in *X. laevis* oocytes. Current-voltage relationships from oocytes injected with 50 ng of *OsHKT2;4* cRNA are shown. During OsHKT2;4-mediated current recordings, the K^+ concentration of the bath solution was increased from 0.3 mM to 10 mM. Note that only the background currents of water-injected control oocytes bathed in a 10 mM K^+ solution were presented as a representative control as no significant difference was found among the three ionic conditions. Currents were recorded from a holding voltage of -40 mV using step commands with 15-mV decrements and error bars represent ± SE (n = 6 for each condition). K^+ was added to the bath solutions as a glutamate salt.

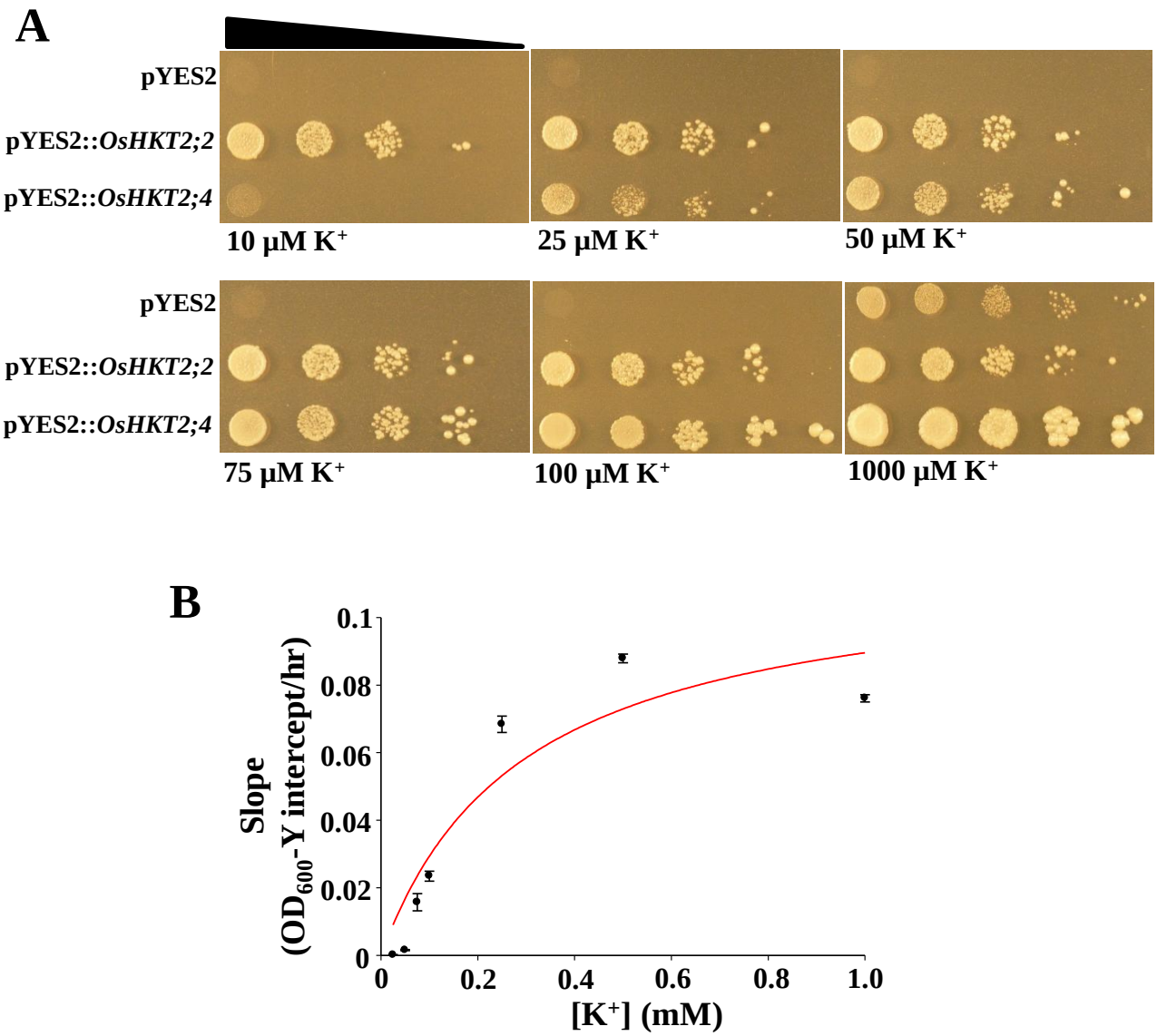

Figure 7. OsHKT2;4 mediates K^+ uptake in yeast cells. (A) CY162 cells harboring pYES2 or the cells expressing OsHKT2;2 or OsHKT2;4 were grown on arginine phosphate (AP) medium supplemented with indicated concentrations of KCl. Each transformant was grown in liquid SC-Ura + 50 mM KCl medium and 1:10 serial dilutions were spotted on plates. All plates were incubated at 30° C for 6 days and photographs were taken afterwards. (B) Concentration-dependent increases in the growth rate of OsHKT2;4-expressing CY162 cells. CY162 cells harboring pYES2 or pYES2::*OsHKT2;4* cDNA were inoculated into liquid AP medium supplemented with either 0.025, 0.05, 0.075, 0.1, 0.25, 0.5 or 1.0 mM KCl at a starting OD_{600} of 0.01. Growth of the cells were monitored and the slope from the linear regression to the growth curves at the logarithmic growth phase of OsHKT2;4-expressing cells were obtained and plotted. The curve in the graph was obtained by a non-linear regression analysis using the Michaelis-Menten curve fitting formula. Three independent experiments were performed and error bars represent ± SD.

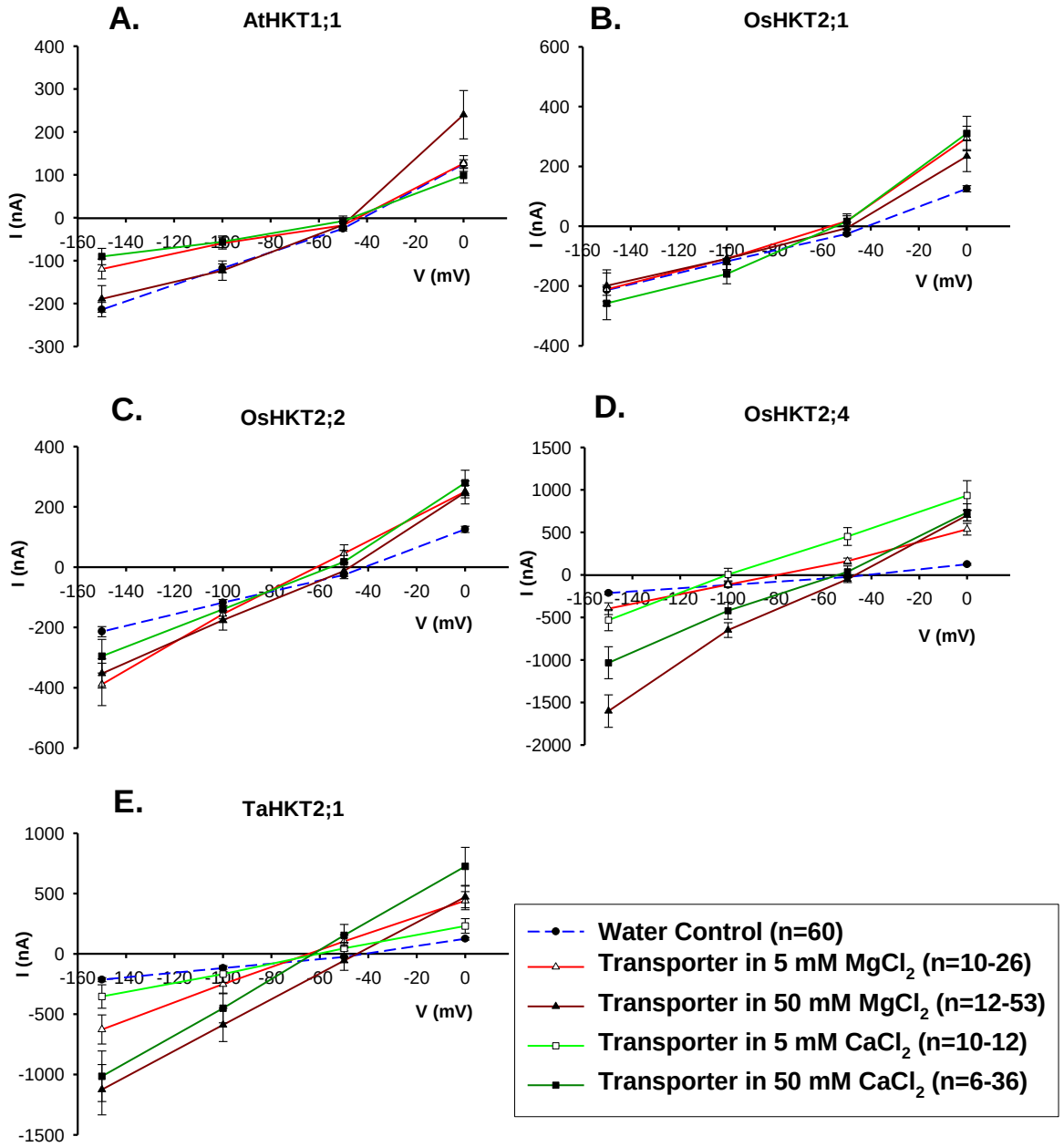

Figure 8. Five HKT family transporters were tested for Mg^{2+} and Ca^{2+} permeability in the presence of 5 mM and 50 mM extracellular concentrations of $MgCl_2$ or $CaCl_2$. AtHKT1;1 and OsHKT2;1 (A,B) showed small changes in the reversal potentials of HKT-mediated currents, even upon extracellular exposure to high 50 mM concentrations of these divalent cations. OsHKT2;2 (C) showed a moderate +13 mV reversal potential shift upon increasing Mg^{2+} from 5 to 50 mM, but the observed current magnitudes were unchanged. OsHKT2;4 and TaHKT2;1 (D,E) exhibited notable shifts in the reversal potentials in response to 50 mM Mg^{2+} concentrations. OsHKT2;4 showed a +33 mV reversal potential shift upon increasing $MgCl_2$ concentration from 5 to 50 mM, and a +45 mV shift for $CaCl_2$ upon increasing concentration from 5 to 50 mM. TaHKT2;1 showed a +20 mV shift for $MgCl_2$ after increasing the bath concentration from 5 to 50 mM, and a -2 mV shift for a 5 to 50 mM $CaCl_2$ increase. Currents were recorded from a holding voltage of -40 mV using a 2.5-second ramp protocol ranging from 0 mV to -150 mV. Specific data points from voltage ramps at -150 mV, -100 mV, -50 mV, and 0 mV were analyzed for the current-voltage graphs, which were used to determine reversal potentials. Error bars represent ± SE (n = 6-53, depending on condition and transporter tested).

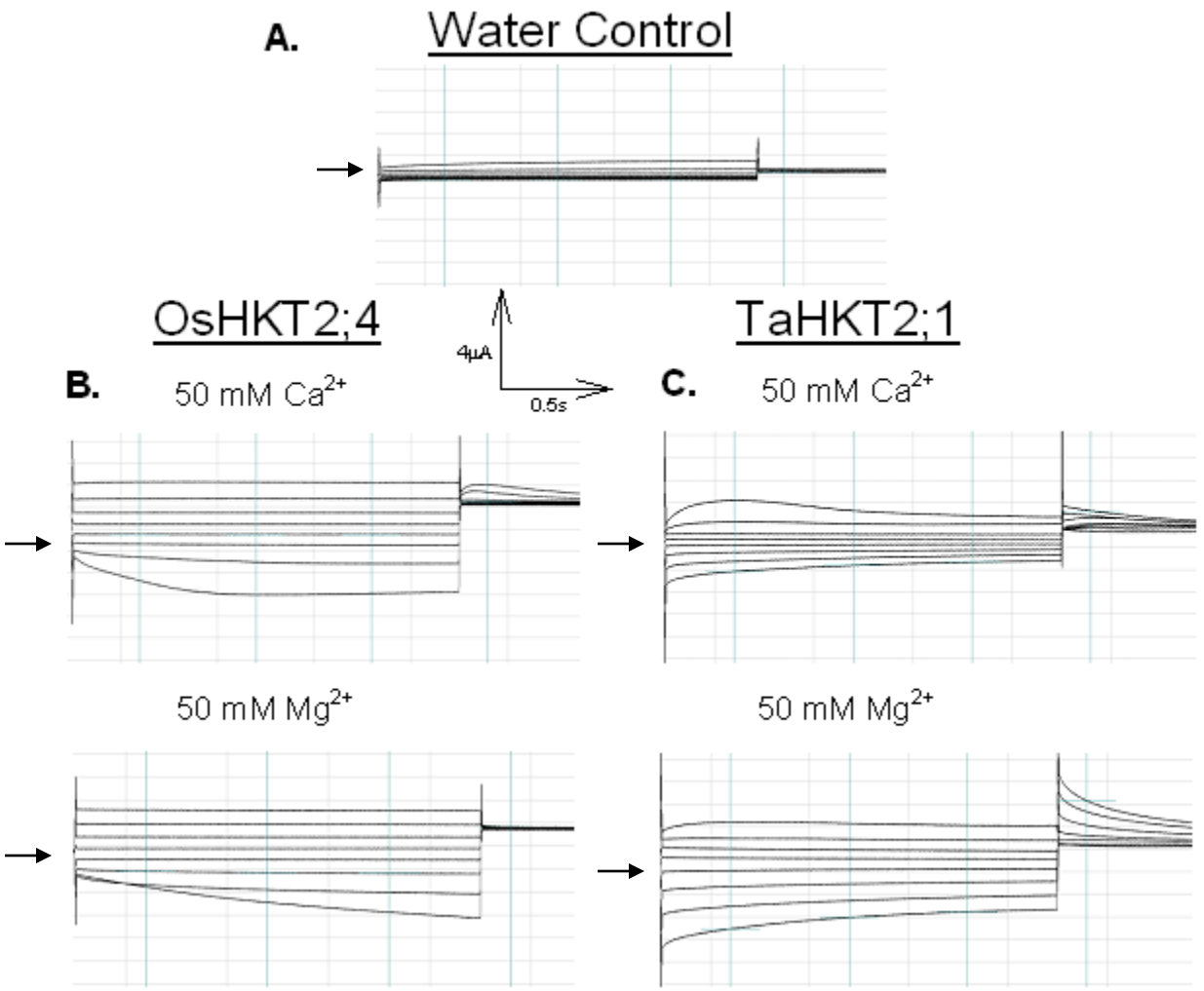

Figure 9. OsHKT2;4 mediates Ca^{2+} and Mg^{2+} transport. The addition of 50 mM Ca^{2+} or Mg^{2+} resulted in large, time dependent inward cation currents for (B) OsHKT2;4 compared to controls (A). (A) Small currents were detected in water-injected control oocytes. A bath solution containing 50 mM $CaCl_2$ was used for the control recording shown. (B) Similar current magnitudes were observed for the 50 mM Ca^{2+} and Mg^{2+} groups in OsHKT2;4. Slow time-dependent activation was commonly observed in OsHKT2;4-injected oocytes during hyperpolarized voltages. (C) Currents recorded in TaHKT2;1-expressing oocytes at the indicated $MgCl_2$ and $CaCl_2$ concentrations. Unlike in OsHKT2;4, slow time-dependent deactivation was commonly observed in TaHKT2;1-injected oocytes during hyperpolarized voltages. Zero current levels are shown by arrows on the left of the recorded currents. Voltage steps ranged from -150 mV to +60 mV in 30 mV increments. The final "tail" voltage at the end of the pulses was +40 mV.

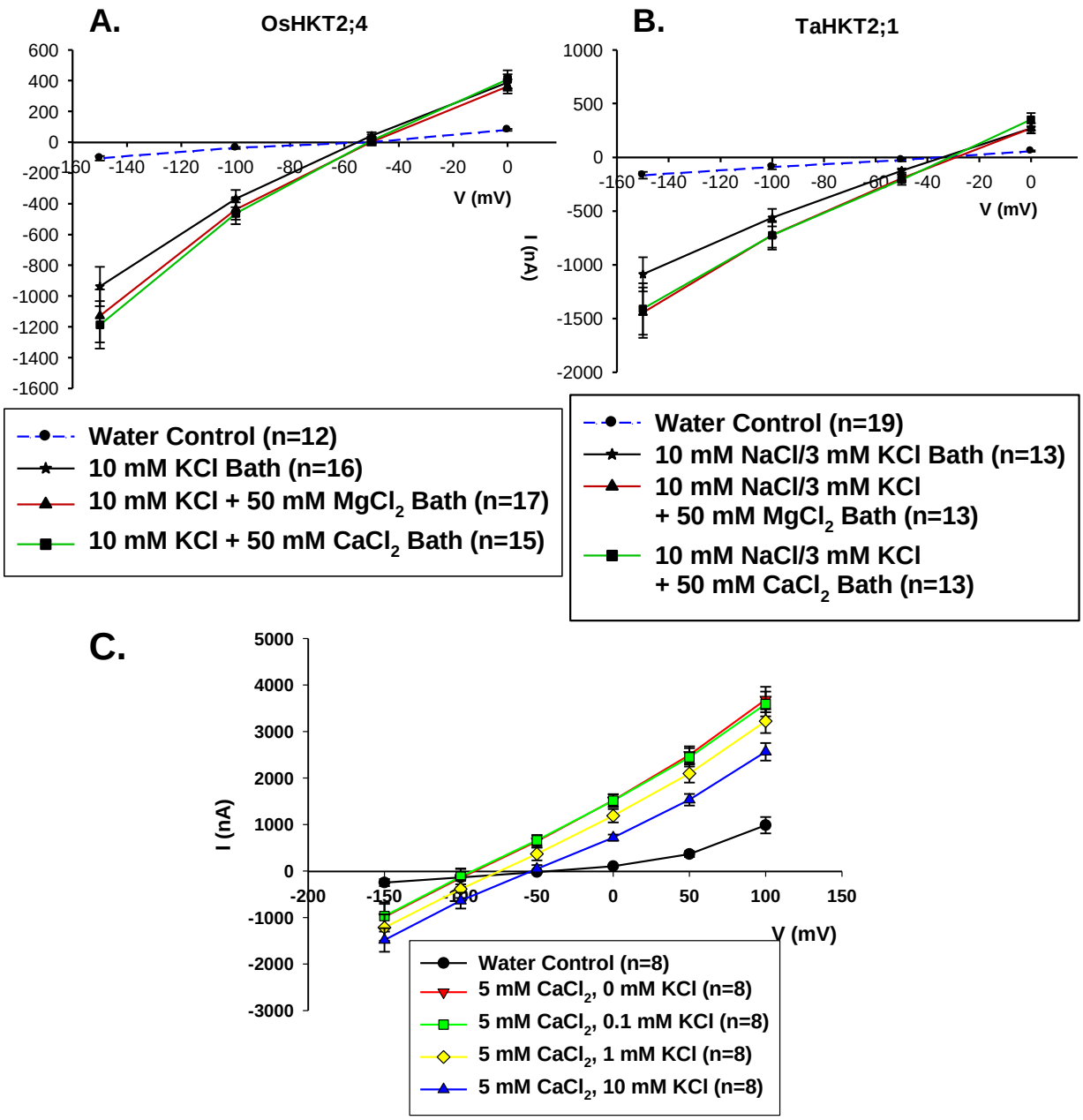

Figure 10. Inhibition of strong Mg^{2+} and Ca^{2+} permeabilities in OsHKT2;4 and TaHKT2;1 was observed in the presence of competing K^+ and Na^+ ions. (A) OsHKT2;4 was analyzed for Mg^{2+} and Ca^{2+} permeabilities in the presence of 10 mM K^+. (B) TaHKT2;1 was analyzed for Mg^{2+} and Ca^{2+} permeabilities in the presence of 10 mM Na^+ and 3 mM K^+. (A) OsHKT2;4 showed a +5 mV reversal potential shift upon adding 50 mM $MgCl_2$ to the 10 mM KCl competition control solution. Addition of $CaCl_2$ also resulted in a small average +4 mV reversal potential shift. (B) TaHKT2;1 exhibited a +6 mV reversal potential shift upon adding 50 mM $MgCl_2$ to the 10 mM NaCl, 3 mM KCl control solution. Addition of 50 mM $CaCl_2$ to the control solution resulted in a smaller +3 mV reversal potential shift. (C) K^+ permeability was observed in the presence of competing Ca^{2+} ions. OsHKT2;4 showed a -2 mV reversal potential shift upon addition of 0.1 mM K^+ to the 5 mM Ca^{2+} bath solution, a +16 mV reversal shift upon addition of 1 mM K^+, and a +36 mV reversal shift upon addition of 10 mM K^+ to the bath solution. Currents were recorded from a holding voltage of -40 mV using step commands with 30-mV decrements and error bars represent ± SE ($n = 12$–19, depending on condition and transporter tested).

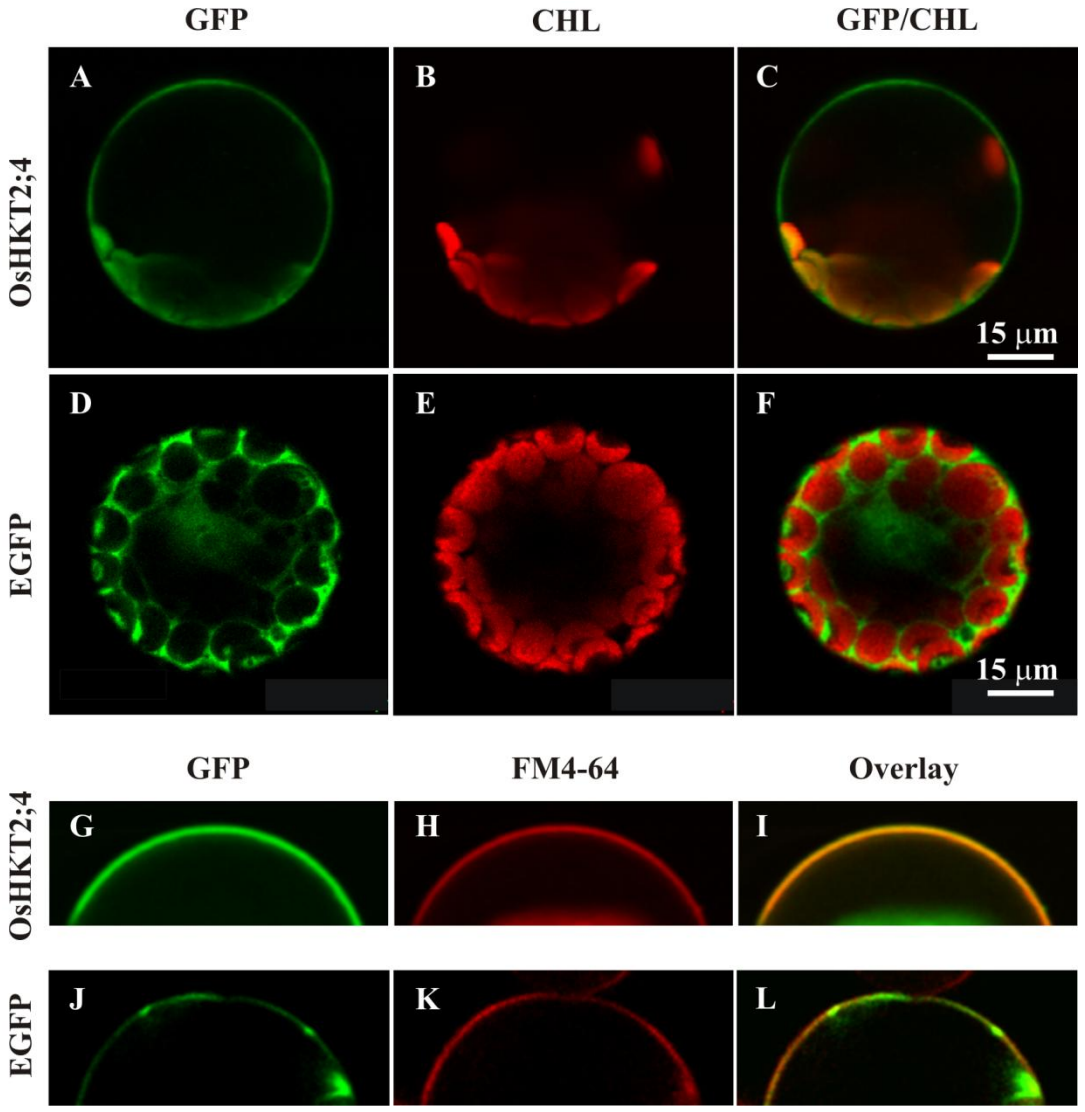

Figure 11. Subcellular localization of EGFP-OsHKT2;4 in *Arabidopsis* mesophyll protoplasts. EGFP-OsHKT2;4 protein was transiently expressed in protoplasts of *Arabidopsis* mesophyll cells under the control of the CaMV 35S promoter. Fluorescence was analyzed by confocal microscopy. (A) EGFP fluorescence (green) from the chimeric EGFP-OsHKT2;4 protein shows fluorescence at the periphery of the protoplast. (B) Chlorophyll auto fluorescence (red) of the same protoplast shown in (A). (C) Overlay image of (A) and (B). (D) Control EGFP fluorescence (green) from the free EGFP. (E) Chlorophyll auto fluorescence (red) of the same protoplast shown in (D). (F) Overlay image of (E) and (D). (G) Confocal EGFP fluorescence (green) image from a focal plane of an EGFP-OsHKT2;4-expressing cell. (H) FM4-64 fluorescence image of the same protoplast shown in (G). (I) Overlay image of (G) and (H). (J) Confocal EGFP fluorescence (green) image of an EGFP-expressing cell. (K) FM4-64 fluorescence image of the same protoplast shown in (J). (L) Overlay image of (J) and (K).